Human-specific derived alleles of *CD33* and other genes protect against postreproductive cognitive decline

Flavio Schwarz[a,b,c,d,1], Stevan A. Springer[a,b,d,1], Tasha K. Altheide[a,b,c,d], Nissi M. Varki[a,b,e], Pascal Gagneux[a,b,e,2], and Ajit Varki[a,b,c,d,2]

[a]Center for Academic Research and Training in Anthropogeny, University of California, San Diego, La Jolla, CA 92093; [b]Glycobiology Research and Training Center, University of California, San Diego, La Jolla, CA 92093; [c]Department of Medicine, University of California, San Diego, La Jolla, CA 92093; [d]Department of Cellular & Molecular Medicine, University of California, San Diego, La Jolla, CA 92093; and [e]Department of Pathology, University of California, San Diego, La Jolla, CA 92093

Edited by Richard G. Klein, Stanford University, Stanford, CA, and approved October 27, 2015 (received for review September 11, 2015)

The individuals of most vertebrate species die when they can no longer reproduce. Humans are a rare exception, having evolved a prolonged postreproductive lifespan. Elders contribute to cooperative offspring care, assist in foraging, and communicate important ecological and cultural knowledge, increasing the survival of younger individuals. Age-related deterioration of cognitive capacity in humans compromises these benefits and also burdens the group with socially costly members. We investigated the contribution of the immunoregulatory receptor CD33 to a uniquely human postreproductive disease, Alzheimer's dementia. Surprisingly, even though selection at advanced age is expected to be weak, a *CD33* allele protective against Alzheimer's disease is derived and unique to humans and favors a functional molecular state of CD33 resembling that of the chimpanzee. Thus, derived alleles may be compensatory and restore interactions altered as a consequence of human-specific brain evolution. We found several other examples of derived alleles at other human loci that protect against age-related cognitive deterioration arising from neurodegenerative disease or cerebrovascular insufficiency. Selection by inclusive fitness may be strong enough to favor alleles protecting specifically against cognitive decline in postreproductive humans. Such selection would operate by maximizing the contributions of postreproductive individuals to the fitness of younger kin.

CD33 | Siglec | postreproductive lifespan | Alzheimer's disease | cognitive capacity

Natural selection operates on differential survival and reproductive success. Accordingly, most vertebrates lose fecundity as they age and die soon after their reproductive periods end. Humans, orcas, and pilot whales are the only vertebrate species known to have prolonged postreproductive lifespans (1, 2). In orcas, older members of the group influence the reproductive success and survival of subsequent generations, implying that activities of postreproductive individuals increase their inclusive fitness (3). Similarly, older humans communicate cultural and ecological information and often make influential decisions within groups and wider social networks. These contributions require maintenance of cognitive capacity (4–6). Dementia (defined as a decline in memory or other thinking skills severe enough to reduce a person's ability to perform everyday activities) negates the informational value of postreproductive individuals, clouds critical decision-making by elders, sometimes results in disruptive behavior, and eventually diverts group resources toward the care of affected individuals. Behaviors and social structures that enhance the effectiveness of postreproductive individuals might therefore be expected to select specifically for the retention of cognitive capacity. In contrast, ancestral alleles that directly enhance survival and reproductive success during fertile years are favored, even if they limit retention of cognitive capacity in postreproductive age and predispose individuals to dementia. Extended postreproductive lifespans may thus evolve as a balance between these two opposing selective forces.

The brains of humans and other related primates differ not only in size and capability but also in their susceptibility to particular diseases. For instance, late-onset Alzheimer's disease (LOAD) is considered to be unique to humans (7). In fact, whereas humans accumulate amyloid beta deposits and neurofibrillary tangles composed of hyperphosphorylated tau protein after age 40 y, postmortem brain samples from age-matched chimpanzees and other great apes do not show the complete pathology of LOAD (8–10). Human-unique neurodegenerative diseases could be byproducts of major differences in brain development that evolved along the human lineage. If so, derived protective alleles may be compensatory and restore functions that were altered as a consequence of human-specific brain evolution.

Genome-wide studies have associated the rs3865444 SNP in the promoter region of the *CD33* gene with LOAD susceptibility (11–13). *CD33* is the canonical member of the family of *CD33*-related *SIGLEC* genes, which have undergone multiple unique genetic and expression changes in the human lineage (14). CD33-related Siglecs are predominantly expressed on cells of the

Significance

Most vertebrates die soon after they stop reproducing, but humans are an exception. Postreproductive humans care for offspring, assist in foraging, and communicate ecological and cultural knowledge, increasing the survival of younger individuals. Loss of cognitive capacity disrupts these benefits and burdens the group with the care of older members. We studied how the immunoregulatory receptor CD33 contributes to Alzheimer's disease, a human-specific postreproductive condition. Surprisingly, a protective *CD33* allele is derived and unique to humans, despite weak direct selection on older individuals. We identified several genes with derived alleles that protect against neurodegenerative disease and cerebrovascular insufficiency in old age. Selection by inclusive fitness may be strong enough to favor alleles that protect against cognitive decline in postreproductive humans.

Author contributions: F.S., S.A.S., P.G., and A.V. designed research; P.G. and A.V. directed research; F.S., S.A.S., and T.K.A. performed research; F.S., S.A.S., T.K.A., and N.M.V. analyzed data; and F.S., S.A.S., T.K.A., N.M.V., P.G., and A.V. wrote the paper.

The authors declare no conflict of interest.

This article is a PNAS Direct Submission.

See Commentary on page 17.

[1]F.S. and S.A.S. contributed equally to this work.

[2]To whom correspondence may be addressed. Email: a1varki@ucsd.edu or pgagneux@ucsd.edu.

This article contains supporting information online at www.pnas.org/lookup/suppl/doi:10.1073/pnas.1517951112/-/DCSupplemental.

innate immune system and modulate cellular reactivity upon recognition of cell surface sialic acids that serve as "self-associated molecular patterns" (15–17). *CD33* encodes a type 1 transmembrane protein with two Ig-like extracellular domains, a single transmembrane span, and two intracellular inhibitory motifs (18). Engagement of sialic acid-containing ligands by the outermost V-set Ig-like domain of CD33 results in the phosphorylation of cytosolic domains, which leads to inhibition of proinflammatory cascades in monocytes and macrophages (19, 20). Human *CD33* produces two alternative splice forms: a full-length CD33M and a minor form CD33m that lacks the exon 2 encoding the V-set domain (Fig. 1*A*) (21, 22). Thus, CD33M and CD33m differ both in molecular weight and in their ability to bind sialic acids.

A series of recent studies has provided a molecular link between the rs3865444 SNP and LOAD. First, CD33 was detected in brain microglia, phagocytic immune cells that respond to cellular damage in the central nervous system (23–25). Then, the rs3865444 SNP associated with LOAD was found to be in complete linkage disequilibrium with rs12459419, a SNP located at the third base pair of *CD33* exon 2 (25, 26). Notably, the rs12459419 SNP was shown to influence the efficiency of exon 2 splicing. Humans homozygous for the LOAD-risk allele marked by rs3865444C have greater cell surface expression of CD33M compared with homozygotes with the LOAD-protective allele rs3865444A (25). Thus, both rs3865444 and rs12459419 polymorphisms predict the ratio of the two CD33 isoforms. Existing studies suggest that CD33M suppresses microglial uptake of amyloid beta peptide, which otherwise accumulates in the central nervous system and contributes to LOAD (27).

Here, we compare the regulation of *CD33* in humans and chimpanzees and assess the splicing and *CD33* expression of alleles that predispose and protect against LOAD. We ask whether the protective allele of CD33 is derived and human-unique and survey alleles of other human genes that are also reported to protect against cognitive decline.

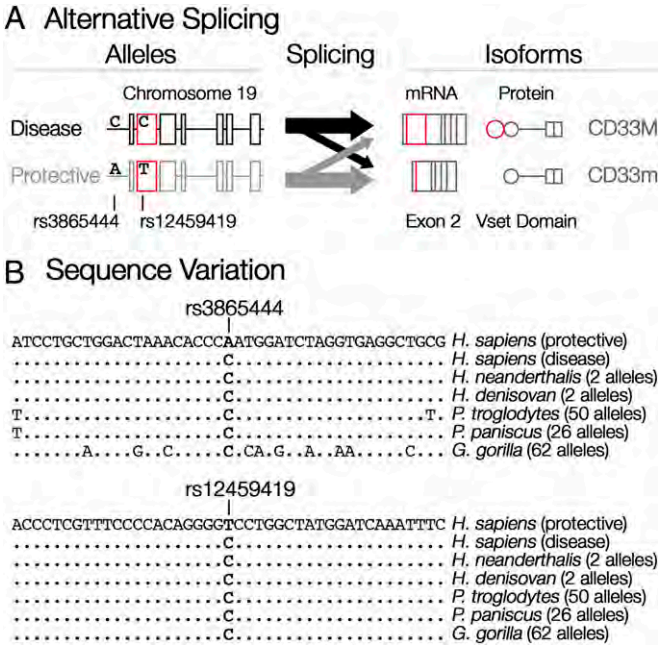

Fig. 1. The LOAD-protective allele rs3865444A is unique to humans. (*A*) Schematic of the human *CD33* genomic region, messenger RNAs generated by alternative splicing, and CD33M and CD33m proteins. Exon 2 encoding the V-set domain is indicated in red. (*B*) Alignments of the sequences surrounding the rs3865444 and rs12459419 SNPs reveal that the rs3865444C and rs12459419C alleles are ancestral. Data for humans are from the 1000 Genomes database. Neanderthal and Denisovan alleles are from the respective genome assemblies, accessed using the University of California, Santa Cruz, genome browser. Primate data are from ref. 28. The number of alleles available for each species is indicated.

Results and Discussion

The Protective CD33 Allele Is Derived in Humans. Because our closest evolutionary relatives do not seem to develop the complete pathology of LOAD, we decided to investigate the allelic state of *CD33* in human and nonhuman primates (Fig. 1*B*). Examination of a recently sequenced dataset of 79 primate genomes (28) showed that chimpanzee, bonobo, and gorilla are fixed for rs3865444C, confirming that the protective allele is derived (in this dataset, orangutans lack information for the *CD33* region). Analysis of the 1000 Genomes dataset shows the rs3865444A LOAD-protective allele is found at an overall frequency of 0.21 in the human population, ranging from 0.05 in Africans to 0.48 in Native Americans (Table 1). Analysis of the available genomic data from Neanderthal and Denisovan genomes showed only the ancestral rs3865444C allele (29, 30). The pattern for rs12459419 is identical: only modern humans have the protective allele, consistent with the observation that these two SNPs are in complete linkage disequilibrium. Thus, the LOAD-protective *CD33* allele represents a derived state in humans, having evolved after our common ancestor with other hominids, and possibly after our common ancestor with Neanderthal and Denisovans 550,000–765,000 y ago (30).

CD33M Is Expressed at Higher Levels in Humans Than in Chimpanzees. We studied expression of CD33 on human and chimpanzee peripheral blood mononuclear cells, using antibodies specific for the two splice forms. Chimpanzee monocytes show lower cell surface expression of CD33M than human monocytes, independent of the allelic state of rs3865444 (Fig. 2*A* and Fig. S1). Immunohistochemistry analysis of brain microsections using antibodies that recognize both CD33 isoforms detected CD33 on human and chimpanzee microglia, but at different levels (Fig. 2*B*). Immunoblot data confirmed a fourfold increase in CD33M expression in human brain with rs3865444C/C compared with chimpanzee brain, whereas expression of CD33m was found to be similar in both species (Fig. 2*B*). Taken together, these data show that two CD33 isoforms are expressed both in human cells and in chimpanzee cells. However, whereas overall CD33M expression is high in humans, CD33M is maintained at lower levels in the chimpanzee. Hence, it appears that at some point after the common ancestor with chimpanzees, the human lineage upregulated CD33M expression as the result of an unknown selective pressure or as a byproduct of other adaptive changes. The increased CD33M expression in humans may have been deleterious in terms of LOAD risk, and an alteration in splicing efficiency to lower the amounts of the CD33M isoform followed.

***CD33* and *APOE* Underwent Comparable Evolutionary Changes.** We noted that the evolutionary history of *CD33* is similar to that of *APOE,* in that both genes have derived alleles that protect from a novel liability that is uniquely human (31–33). The *APOE* gene, which encodes for the plasma protein APOE, is polymorphic in humans. The three isoforms (ε2, ε3, and ε4) have a distinct affinity for lipoprotein particles (34). Carriers of the minor ε4 allele have higher levels of total cholesterol and accumulate atherosclerotic plaques in their arteries, leading to increased risks for cardiovascular disease, stroke, vascular dementia, and LOAD (31). The three alleles differ at two key nonsynonymous sites, resulting in amino acid differences at positions 112 and 158. Although the APOE of nonhuman mammals (including great apes) and the human ε4 allele share the same residues at 112 and 158, studies of transgenic mice indicate that a threonine at position 61 in the APOE of nonhuman primates causes binding preferences that are functionally similar to the derived human ε3

Table 1. Examples of genes affecting cognitive functions in postreproductive age exhibiting disease-protective alleles uniquely in humans

Gene	Associated disease	SNP	Derived allele	Frequency of derived allele*						Reference
				ALL	AFR	AMR	ASN	EUR	SAS	
CD33	LOAD	rs3865444	A	0.21	0.05	0.48	0.19	0.31	0.16	12
		rs12459419	T	0.21	0.05	0.48	0.19	0.31	0.16	25, 26
APOE	LOAD, cardiovascular disease	rs7412	T	0.08	0.10	0.05	0.10	0.06	0.04	31
		rs429358	T	0.85	0.73	0.90	0.91	0.84	0.91	
AGT	Sodium retention, sodium-sensitive hypertension	rs699	A	0.29	0.10	0.36	0.15	0.59	0.36	44, 45
SCG2	Hypertension	rs1017448	G	0.88	0.63	0.95	0.96	0.98	0.97	46
CAPN10	Type II diabetes	rs2975760	T	0.88	0.97	0.87	0.91	0.84	0.79	41, 76
TCF7L2	Type II diabetes	rs7903146	C	0.77	0.74	0.77	0.98	0.68	0.70	47, 77
EBF1[†]	Cardiovascular disease	rs2149954	C	0.66	0.61	0.73	0.77	0.65	0.59	78
COX-2	Myocardial infarction and ischemic stroke	rs20417	C	0.80	0.65	0.79	0.96	0.85	0.81	79
CYP3A5	Salt retention and hypertension	rs776746[‡]	C	0.62	0.18	0.80	0.71	0.94	0.67	80
PPARG	Type II diabetes	rs1801282	G	0.07	0.01	0.12	0.03	0.12	0.12	39
PON1	Dementia	rs2618516	T	0.34	0.26	0.24	0.30	0.38	0.52	81

AFR, African; AMR, American; ASN, East Asian; EUR, European; SAS, South Asian.
*Allele frequencies are from the 1000 Genomes database.
[†]302 kb downstream.
[‡]Most common nonfunctional.

allele (35). Thus, although human ε4 is the ancestral allele, it appeared sometime before the common ancestor of modern humans, possibly in relationship to higher lipid consumption associated with increased access to meat or marrow in the genus *Homo* (36). Evolutionary changes in both *CD33* and *APOE* along the human lineage caused detrimental effects on the cognition of older individuals. The direction of the compensatory changes in the derived alleles is also noteworthy: in both genes, the new alleles seem to restore former interactions (lower levels of immune inhibitory CD33 and a functionally apelike APOE protein sequence in human ε3). The derived protective alleles are found to be polymorphic in all populations, which suggests they do not have direct advantageous effects on the fitness of young individuals. Their direct effects on young individuals could be neutral or deleterious and could be offset by the helpful behaviors of postreproductive individuals that carry a protective allele. In humans, these benefits could be directed actively, by kin-directed nepotistic behavior, or probabilistically, by social structures that favor interactions among old and young family members. Thus, selection by inclusive fitness may be capable of favoring alleles that protect against cognitive decline in late life, despite weak direct selection on the phenotypes of older individuals themselves.

Many Other Genes Underlying Cognitive Decline Have Derived Protective Alleles. LOAD risk and progression are aggravated by vascular dementia, which is linked to risk factors such as hypertension, type 2 diabetes dyslipidemias, and obesity (37). Indeed, it is difficult to untangle the pathologies of Alzheimer's disease and vascular dementia in older individuals. Even in Alzheimer's disease, vascular pathology such as small vessel disease may have a greater influence on disease course than amyloid itself, especially in older individuals (38). These observations prompted us to extend our search for genes with human-derived alleles with potential protective properties against cognitive decline and vascular dementia in postreproductive humans (Table 1). PPARG (peroxisome proliferator-activated receptor gamma) is a nuclear hormone receptor that regulates adipogenesis. A modest but significant increase in diabetes risk is associated with the more common allele P12, whereas the protective A12 allele is derived (39, 40). Similarly, *CAPN10* encodes a member of the calpain-like cysteine protease family that regulates blood glucose levels. The derived allele at SNP 44 (rs2975760) protects against type II diabetes mellitus (41). In this case, population genetic analyses reveal a significant deficit of variation in the haplotypes surrounding the derived allele, suggesting it is being driven to high frequency by positive selection (42, 43). Variants that control sodium homeostasis show similar patterns: ancestral alleles increase risk of hypertension, whereas the derived alleles are protective. For instance, the geographic distribution of the A(-6)G variant in the promoter region of human angiotensinogen (*AGT*) suggests the G(-6) variant is selectively advantageous outside Africa. The derived allele is present at higher frequency in Asians and Europeans, but the ancestral (sodium-conserving) alleles are more prevalent in Africans (44, 45). A regulatory polymorphism in Secretogranin II (*SCG2*) associates with hypertension in African Americans, with a derived protective allele (46). The T allele of the transcription factor-7-like 2 (*TCF7L2*) gene is associated with impaired insulin secretion and enhanced hepatic glucose production (47). Positive selection has driven derived haplotypes at this locus to near fixation in East Asians. Thus, many genes involved in management of cognitive functions appeared to have evolved protective alleles that remain polymorphic in the human lineage.

The Origins of Some Derived Protective Alleles May Predate the Origin of Modern Humans. It has been proposed that derived protective alleles arose and underwent selection primarily after human populations became agrarian, with the changes in selection caused by a sedentary lifestyle and increased consumption of carbohydrate- and lipid-rich diets (48, 49). This scenario clearly holds for lactase persistence and may also be true of some of the derived alleles in Table 1. However, surveys of the literature, and our current analyses using several different population-level metrics (F_{ST}, Rbp, iHS, Tajima's D, and Fay and Wu's H; Dataset S1), indicate that these genes do not consistently show signs of recent selection. In the 1000 Genomes data, some do show evidence of population structure and of possible deviations from neutrality; others appear to be evolving neutrally. Moreover, all the protective derived alleles in Table 1 are present in African populations, on the continent where modern humans originated and where contemporary nonagrarian societies persist. If inclusive selection operated on these other derived protective alleles, it may have been most effective near the origin of behaviorally modern humans ~100,000 y ago, a depth of time at which clear genomic signatures of selection and selective sweeps are degraded beyond recognition with existing statistical methods (48–50).

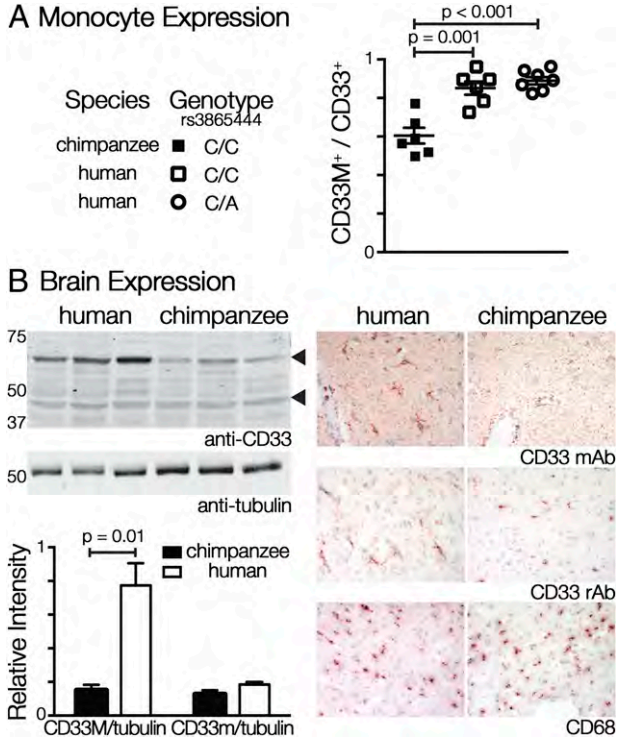

Fig. 2. Full-length CD33M is expressed at higher levels in humans compared with in chimpanzee. (*A*) CD33M is expressed at higher levels on the cell surface of human peripheral blood monocytes. $CD33M^+/CD33^+$ values reflect the ratio of WM53/HIM3.3 positive cells. The rs3865444 allelic state is indicated. Error bars reflect mean ± SEM. *P* values were calculated with an unpaired Student's *t* test. (*B*) CD33M is expressed at higher levels in human brain, whereas CD33m is expressed at comparable levels in human and chimpanzee. Human samples were from homozygous C/C subjects for the rs3865444 SNP. Tubulin is used for normalization of signals. Error bars reflect mean ± SEM; $n = 3$. *P* values were calculated with an unpaired Student's *t* test. Immunohistochemistry shows expression of CD33 both in chimpanzee and human brain. Mouse monoclonal (mAb) and rabbit polyclonal (rAb) CD33 antibodies detect both CD33 forms. CD68 is used as a marker for microglia.

Conclusions and Perspectives

Survival beyond a fertile age is not a recent phenomenon in human groups, as hunter–gatherer populations exhibit aging structures in which about a third of the females are postreproductive (51). In contrast, chimpanzee females rarely live past fertile years, even when accorded full veterinary care in captivity (5, 52, 53). It has been suggested that the cooperative child-rearing in humans is crucially tied to the survival of grandmothers (5, 54) and also greatly contributed to the shortening of interbirth interval in humans (3–4 y compared with more than 4 y in chimpanzees) (55, 56). Unlike chimpanzees, young humans are unable to feed themselves until long after they reach weaning age and critically depend on the help and support of group members other than their mothers. Cooperative breeding played a key role in human cognitive evolution (57), and selection for grandmothering could have propelled the evolution of postmenopausal longevity, setting the social context for the subsequent evolution of many other features in our lineage (5, 54, 58–60). For humans, however, intergenerational information transfer is also an important factor for the survival of individuals, groups, and larger social networks characteristic of foraging societies (61). Such information transfer could enhance inclusive fitness via resource sharing and reduced mortality of younger individuals (62–64).

Antagonistic pleiotropy is considered a key mechanism in the evolution of senescence (65), as genes strongly selected for their positive effects early in life via differential survival or reproductive success can have deleterious (pleiotropic) effects later in life, when natural selection is weak or absent. Derived alleles that protect against cognitive decline during a prolonged postreproductive period could result from kin selection late in life through increased survival of younger kin. Such alleles would operate by maintaining the cognitive capacity of grandmothers, as well as of active elderly decision makers and transmitters of valuable cultural information. Both of these features are apparently unique to humans compared with other primates. Indeed, the onset of dementia in otherwise physically fit humans would have a detrimental effect on these functions not only because of the dysfunctional and sometimes disruptive behavior of affected elders but also because of the time and resources eventually needed to care for older individuals whose decision making is compromised.

Taken together, these data indicate that the existence of a postreproductive lifespan in humans may be supported by selection to maintain cognitive function in older individuals. It would be interesting to search for similar derived alleles in the two mammalian species of toothed whales also known to have prolonged postreproductive lifespans (3, 66). Interestingly, in at least one instance (*Orcinus orca*; Orcas, or killer whales), it has been suggested that ecological knowledge and leadership may have led to the evolution of menopause (3). Postmenopausal female killer whales lead foraging groups, and their leadership is most significant for the survival of the group when food is scarce (67). Helping by older female orcas results in differential survival of their male offspring, indicating kinship dynamics and inclusive fitness effects.

The evolutionary window in which cognition-based selection could operate in humans likely opened with the development of linguistic capabilities and the capacity for cumulative culture and shared intentionality. This indicates a time depth of >100 kya, which limits the potential to detect selective sweeps with existing statistical methods. However, polymorphic protective alleles do exist, and there could be ongoing selection for alleles that protect against cognitive decline in contemporary human populations. Blue zones are populations in which extreme human longevity occurs in the absence of modern medicine (68, 69). It is interesting that in these populations, there tends to be no "retirement" age: older individuals continue to be active, functional members of society.

Materials and Methods

***CD33* rs3865444 Genotyping.** Genomic DNA was extracted from blood and tissues with a DNeasy Blood & Tissue Kit (Qiagen). The allelic state of rs3865444 was defined by NcoI digestion of a 421-bp fragment amplified from genomic DNA, using primers 5′-GCGAACCCCATGTCTAAA-3′ and 5′-CCTACCTCCCTCTGTGCC-5′ (70).

CD33 Expression on Blood Monocytes. Chimpanzee blood samples were collected as extra tubes only during routine noninvasive health screens of chimpanzee subjects at the Yerkes National Primate Center, Emory University, Atlanta [supported by NIH Base Grant ORIP/OD P51OD011132; routine collection covered under local institutional review board (IRB) approval by Emory University]. All collections were made prior to the September 15, 2015 designation of captive chimpanzees as endangered species. Chimpanzee blood samples were shipped overnight on ice to the University of California, San Diego. Human blood was collected at about the same time into identical tubes from healthy volunteer donors (following informed consent, under the approval from the University of California, San Diego Human Subjects IRB), and stored overnight on ice, to ensure similar treatment conditions prior to analysis. All health and safety issues related to handling of human and nonhuman primate samples are covered by an institutional biosafety approval from the University of California, San Diego Environmental Health and Safety Committee. All individuals who handle the samples receive the required training regarding precautions for blood-borne pathogens. Peripheral blood mononuclear cells were isolated by centrifugation over Ficoll-Paque Premium (GE Healthcare). Contaminating red blood cells were lysed by incubation in

ACK buffer (Gibco, Life Technologies). Cells were stained with an APC-conjugated anti-CD33 antibodies clone WM53 (BD Biosciences) and a FITC-conjugated anti-CD33 antibodies clone HIM3.4 (Biolegend), or isotype control antibodies. CD33 expression was measured with a BD FACSCalibur (BD Biosciences). Data were analyzed with FlowJo.

Immunohistochemistry. Frozen or paraffin-embedded samples of human brain were obtained from the National Cancer Institute-funded Co-operative Human Tissue Network. Frozen or paraffin embedded samples from chimpanzee brains were obtained from the Yerkes Primate Research Foundation. Frozen sections were blocked for endogenous peroxidases and endogenous biotin and were overlaid with control mouse IgGs (Abcam), mouse anti-CD68 (AbD Serotec), rabbit IgGs (Jackson ImmunoResearch Laboratories, Inc.), or rabbit anti-CD33 polyclonal antibodies (Santa Cruz Biotechnology, Inc.), followed by detection using appropriate secondary reagents, color developed using the AEC substrate (Vector Laboratories), followed with Mayer's nuclear counterstain, using established protocols. Deparaffinized tissue sections were treated with antigen retrieval in Decloaking Chamber (Biocare) and overlaid with mouse anti-CD33 monoclonal antibodies (clone PWS44; Leica Biosystems Inc.) overnight at 4 °C in a humid chamber. Sections were incubated with biotinylated anti-mouse IgG antibodies, HRP-conjugated streptavidin, biotinyl tyramide enhancement, and HRP-conjugated streptavidin, followed by AEC substrate. Nuclei were counterstained with Mayer's hematoxylin.

Immunoblot. Frozen brain samples were homogenized in lysis buffer [1% (vol/vol) Nonidet P-40, 20 mM Tris at pH 8, 150 mM NaCl]. Lysates were spun twice at 20,000 × *g*. Protein concentration of the supernatant was measured with a BCA kit (Pierce). Proteins were separated by SDS/PAGE and transferred to nitrocellulose membrane. Membranes were incubated with rabbit anti-CD33 (St Cruz Biotechnology, Inc.) or mouse anti-tubulin antibodies (Sigma), as well as secondary antibodies (LI-COR). Signals were acquired with an Odyssey instrument (LI-COR) and analyzed by Image Studio software (LI-COR).

Statistical Analysis. Unpaired Student's *t* test was used for comparisons involving two groups. Prism 6 Program (GraphPad) was used for most of the statistical analyses.

Genomic Data. Human genomes were accessed from the 1000 Genomes Project server (www.1000genomes.org/), using tabix to extract regions in variant call format (VCF 4.1) (71). Neanderthal and Denisovan VCFs were downloaded from their respective servers (Neanderthal, cdna.eva.mpg.de/neandertal/altai/AltaiNeandertal/VCF/; Denisovan, cdna.eva.mpg.de/denisova/VCF/hg19_1000g/) (29, 30). Primate VCFs were downloaded from the Great Ape Genome Project server (biologiaevolutiva.org/greatape/) (28). Bed coordinates defining the genomic regions surrounding CD33 and other genes were retrieved using the University of California, Santa Cruz, genome browser (72). Primate VCFs are referenced to hg18, bed coordinates were lifted to hg19 using CrossMap (crossmap.sourceforge.net/). New coordinates were checked against hg19 and corrected by hand when necessary. Variants in each region of each species were extracted with vcftools (73), and variants of each CD33 SNP were called directly from each file.

Polymorphism Tests. Bed coordinates of the loci in Table 1 were retrieved from build hg19, using the University of California, Santa Cruz, Genome Browser. A region containing each gene, plus 100 kb upstream and 100 kb downstream, was retrieved in VCF format from the 1000 Genomes Project database, using tabix. Patterns of polymorphism at each gene and its surrounding region were analyzed for each population and each region (as defined by the 1000 Genomes Project), using the selectionTools pipeline and custom Perl scripts (74). Several statistical tests were evaluated: frequency-based methods (Tajima's D, Fay and Wu's H); linkage disequilibrium-based methods (Rsb, iHs); and population differentiation-based methods (F_{ST}). Each is suited to detecting selection at different timescales. Frequency-based and population differentiation-based methods are better suited to detecting events farther in the past than linkage disequilibrium-based methods (75). Outputs from selectionTools were formatted with custom Perl scripts and visualized in R as heatmaps. Plots were examined for evidence of deviation from the null expectation. The values of each test statistic from the 200 kb surrounding the gene of interest were used to generate histograms that describe the empirical null expectation. Test statistic values from within each gene itself were compared with this expectation to look for statistical outliers whose positions lie within in the gene of interest.

ACKNOWLEDGMENTS. We thank Andrea Garcia-Bingman for help with immunohistochemistry and the members of the A.V. and P.G. groups for suggestions. This work was supported by grants from the National Institutes of Health (P01HL107150 to A.V. and R01GM095882 to P.G.) and by the Harold and Leila Mathers Foundation.

1. Croft DP, Brent LJ, Franks DW, Cant MA (2015) The evolution of prolonged life after reproduction. *Trends Ecol Evol* 30(7):407–416.
2. Jones OR, et al. (2014) Diversity of ageing across the tree of life. *Nature* 505(7482): 169–173.
3. Brent LJ, et al. (2015) Ecological knowledge, leadership, and the evolution of menopause in killer whales. *Curr Biol* 25(6):746–750.
4. Johnstone RA, Cant MA (2010) The evolution of menopause in cetaceans and humans: The role of demography. *Proc Biol Sci* 277(1701):3765–3771.
5. Lahdenperä M, Lummaa V, Helle S, Tremblay M, Russell AF (2004) Fitness benefits of prolonged post-reproductive lifespan in women. *Nature* 428(6979):178–181.
6. Fox M, et al. (2010) Grandma plays favourites: X-chromosome relatedness and sex-specific childhood mortality. *Proc Biol Sci* 277(1681):567–573.
7. Rapoport SI (1989) Hypothesis: Alzheimer's disease is a phylogenetic disease. *Med Hypotheses* 29(3):147–150.
8. Gearing M, Rebeck GW, Hyman BT, Tigges J, Mirra SS (1994) Neuropathology and apolipoprotein E profile of aged chimpanzees: Implications for Alzheimer disease. *Proc Natl Acad Sci USA* 91(20):9382–9386.
9. Rosen RF, et al. (2008) Tauopathy with paired helical filaments in an aged chimpanzee. *J Comp Neurol* 509(3):259–270.
10. Finch CE, Austad SN (2015) Commentary: Is Alzheimer's disease uniquely human? *Neurobiol Aging* 36(2):553–555.
11. Hollingworth P, et al.; Alzheimer's Disease Neuroimaging Initiative; CHARGE consortium; EADI1 consortium (2011) Common variants at ABCA7, MS4A6A/MS4A4E, EPHA1, CD33 and CD2AP are associated with Alzheimer's disease. *Nat Genet* 43(5): 429–435.
12. Naj AC, et al. (2011) Common variants at MS4A4/MS4A6E, CD2AP, CD33 and EPHA1 are associated with late-onset Alzheimer's disease. *Nat Genet* 43(5):436–441.
13. Bertram L, et al. (2008) Genome-wide association analysis reveals putative Alzheimer's disease susceptibility loci in addition to APOE. *Am J Hum Genet* 83(5): 623–632.
14. Schwarz F, Fong JJ, Varki A (2015) Human-specific evolutionary changes in the biology of siglecs. *Adv Exp Med Biol* 842:1–16.
15. Angata T, Margulies EH, Green ED, Varki A (2004) Large-scale sequencing of the CD33-related Siglec gene cluster in five mammalian species reveals rapid evolution by multiple mechanisms. *Proc Natl Acad Sci USA* 101(36):13251–13256.
16. Macauley MS, Crocker PR, Paulson JC (2014) Siglec-mediated regulation of immune cell function in disease. *Nat Rev Immunol* 14(10):653–666.
17. Varki A (2011) Since there are PAMPs and DAMPs, there must be SAMPs? Glycan "self-associated molecular patterns" dampen innate immunity, but pathogens can mimic them. *Glycobiology* 21(9):1121–1124.
18. Freeman SD, Kelm S, Barber EK, Crocker PR (1995) Characterization of CD33 as a new member of the sialoadhesin family of cellular interaction molecules. *Blood* 85(8): 2005–2012.
19. Lajaunias F, Dayer JM, Chizzolini C (2005) Constitutive repressor activity of CD33 on human monocytes requires sialic acid recognition and phosphoinositide 3-kinase-mediated intracellular signaling. *Eur J Immunol* 35(1):243–251.
20. Ishida A, et al. (2014) Negative regulation of Toll-like receptor-4 signaling through the binding of glycosylphosphatidylinositol-anchored glycoprotein, CD14, with the sialic acid-binding lectin, CD33. *J Biol Chem* 289(36):25341–25350.
21. Hernández-Caselles T, et al. (2006) A study of CD33 (SIGLEC-3) antigen expression and function on activated human T and NK cells: Two isoforms of CD33 are generated by alternative splicing. *J Leukoc Biol* 79(1):46–58.
22. Pérez-Oliva AB, et al. (2011) Epitope mapping, expression and post-translational modifications of two isoforms of CD33 (CD33M and CD33m) on lymphoid and myeloid human cells. *Glycobiology* 21(6):757–770.
23. Griciuc A, et al. (2013) Alzheimer's disease risk gene CD33 inhibits microglial uptake of amyloid beta. *Neuron* 78(4):631–643.
24. Bradshaw EM, et al.; Alzheimer Disease Neuroimaging Initiative (2013) CD33 Alzheimer's disease locus: Altered monocyte function and amyloid biology. *Nat Neurosci* 16(7):848–850.
25. Malik M, et al. (2013) CD33 Alzheimer's risk-altering polymorphism, CD33 expression, and exon 2 splicing. *J Neurosci* 33(33):13320–13325.
26. Raj T, et al. (2014) CD33: Increased inclusion of exon 2 implicates the Ig V-set domain in Alzheimer's disease susceptibility. *Hum Mol Genet* 23(10):2729–2736.
27. Mawuenyega KG, et al. (2010) Decreased clearance of CNS beta-amyloid in Alzheimer's disease. *Science* 330(6012):1774.
28. Prado-Martinez J, et al. (2013) Great ape genetic diversity and population history. *Nature* 499(7459):471–475.
29. Meyer M, et al. (2012) A high-coverage genome sequence from an archaic Denisovan individual. *Science* 338(6104):222–226.
30. Prüfer K, et al. (2014) The complete genome sequence of a Neanderthal from the Altai Mountains. *Nature* 505(7481):43–49.
31. Finch CE, Sapolsky RM (1999) The evolution of Alzheimer disease, the reproductive schedule, and apoE isoforms. *Neurobiol Aging* 20(4):407–428.

32. Raichlen DA, Alexander GE (2014) Exercise, APOE genotype, and the evolution of the human lifespan. *Trends Neurosci* 37(5):247–255.
33. Mahley RW, Huang Y (2012) Apolipoprotein e sets the stage: Response to injury triggers neuropathology. *Neuron* 76(5):871–885.
34. Fullerton SM, et al. (2000) Apolipoprotein E variation at the sequence haplotype level: Implications for the origin and maintenance of a major human polymorphism. *Am J Hum Genet* 67(4):881–900.
35. Raffai RL, Dong LM, Farese RV, Jr, Weisgraber KH (2001) Introduction of human apolipoprotein E4 "domain interaction" into mouse apolipoprotein E. *Proc Natl Acad Sci USA* 98(20):11587–11591.
36. Finch CE, Stanford CB (2004) Meat-adaptive genes and the evolution of slower aging in humans. *Q Rev Biol* 79(1):3–50.
37. Iadecola C (2013) The pathobiology of vascular dementia. *Neuron* 80(4):844–866.
38. Prins ND, Scheltens P (2015) White matter hyperintensities, cognitive impairment and dementia: An update. *Nat Rev Neurol* 11(3):157–165.
39. Altshuler D, et al. (2000) The common PPARgamma Pro12Ala polymorphism is associated with decreased risk of type 2 diabetes. *Nat Genet* 26(1):76–80.
40. McCarthy MI (2004) Progress in defining the molecular basis of type 2 diabetes mellitus through susceptibility-gene identification. *Hum Mol Genet* 13(Spec No 1): R33–R41.
41. Weedon MN, et al. (2003) Meta-analysis and a large association study confirm a role for calpain-10 variation in type 2 diabetes susceptibility. *Am J Hum Genet* 73(5): 1208–1212.
42. Vander Molen J, et al. (2005) Population genetics of CAPN10 and GPR35: Implications for the evolution of type 2 diabetes variants. *Am J Hum Genet* 76(4):548–560.
43. Fullerton SM, et al. (2002) Geographic and haplotype structure of candidate type 2 diabetes susceptibility variants at the calpain-10 locus. *Am J Hum Genet* 70(5): 1096–1106.
44. Nakajima T, et al. (2004) Natural selection and population history in the human angiotensinogen gene (AGT): 736 complete AGT sequences in chromosomes from around the world. *Am J Hum Genet* 74(5):898–916.
45. Inoue I, et al. (1997) A nucleotide substitution in the promoter of human angiotensinogen is associated with essential hypertension and affects basal transcription in vitro. *J Clin Invest* 99(7):1786–1797.
46. Wen G, et al. (2007) An ancestral variant of Secretogranin II confers regulation by PHOX2 transcription factors and association with hypertension. *Hum Mol Genet* 16(14):1752–1764.
47. Helgason A, et al. (2007) Refining the impact of TCF7L2 gene variants on type 2 diabetes and adaptive evolution. *Nat Genet* 39(2):218–225.
48. Babbitt CC, Warner LR, Fedrigo O, Wall CE, Wray GA (2011) Genomic signatures of diet-related shifts during human origins. *Proc Biol Sci* 278(1708):961–969.
49. Jeong C, Di Rienzo A (2014) Adaptations to local environments in modern human populations. *Curr Opin Genet Dev* 29:1–8.
50. Sabeti PC, et al. (2006) Positive natural selection in the human lineage. *Science* 312(5780):1614–1620.
51. Blurton Jones NG, Hawkes K, O'Connell JF (2002) Antiquity of postreproductive life: Are there modern impacts on hunter-gatherer postreproductive life spans? *Am J Hum Biol* 14(2):184–205.
52. Hill K, et al. (2001) Mortality rates among wild chimpanzees. *J Hum Evol* 40(5): 437–450.
53. Herndon JG, et al. (2012) Menopause occurs late in life in the captive chimpanzee (Pan troglodytes). *Age (Dordr)* 34(5):1145–1156.
54. Hawkes K, Coxworth JE (2013) Grandmothers and the evolution of human longevity: A review of findings and future directions. *Evol Anthropol* 22(6):294–302.
55. Key CA (2000) The evolution of human life history. *World Archaeol* 31(3):329–350.
56. Cant MA, Johnstone RA (2008) Reproductive conflict and the separation of reproductive generations in humans. *Proc Natl Acad Sci USA* 105(14):5332–5336.
57. Hrdy SB (2009) *Mothers and others: The evolutionary origins of mutual understanding* (Belknap Press of Harvard University Press, Cambridge, MA).
58. Hawkes K, O'Connell JF, Jones NG, Alvarez H, Charnov EL (1998) Grandmothering, menopause, and the evolution of human life histories. *Proc Natl Acad Sci USA* 95(3): 1336–1339.
59. Kim PS, Coxworth JE, Hawkes K (2012) Increased longevity evolves from grandmothering. *Proc Biol Sci* 279(1749):4880–4884.
60. Kim PS, McQueen JS, Coxworth JE, Hawkes K (2014) Grandmothering drives the evolution of longevity in a probabilistic model. *J Theor Biol* 353:84–94.
61. Hill KR, Wood BM, Baggio J, Hurtado AM, Boyd RT (2014) Hunter-gatherer inter-band interaction rates: Implications for cumulative culture. *PLoS One* 9(7):e102806.
62. Kaplan H, Gurven M, Winking J, Hooper PL, Stieglitz J (2010) Learning, menopause, and the human adaptive complex. *Ann N Y Acad Sci* 1204:30–42.
63. Gurven M, Stieglitz J, Hooper PL, Gomes C, Kaplan H (2012) From the womb to the tomb: The role of transfers in shaping the evolved human life history. *Exp Gerontol* 47(10):807–813.
64. Lee R (2008) Sociality, selection, and survival: Simulated evolution of mortality with intergenerational transfers and food sharing. *Proc Natl Acad Sci USA* 105(20): 7124–7128.
65. GC W (1957) Pleiotropy, Natural Selection, and the Evolution of Senescence. *Evolution* 11:398–411.
66. Lahdenperä M, Mar KU, Lummaa V (2014) Reproductive cessation and post-reproductive lifespan in Asian elephants and pre-industrial humans. *Front Zool* 11:54.
67. Whitehead H (2015) Life history evolution: What does a menopausal killer whale do? *Curr Biol* 25(6):R225–R227.
68. Pes GM, et al. (2015) Male longevity in Sardinia, a review of historical sources supporting a causal link with dietary factors. *Eur J Clin Nutr* 69(4):411–418.
69. Soriano JB, et al. (2014) Description of extreme longevity in the Balearic Islands: Exploring a potential Blue Zone in Menorca, Spain. *Geriatr Gerontol Int* 14(3):620–627.
70. Deng YL, et al. (2012) The prevalence of CD33 and MS4A6A variant in Chinese Han population with Alzheimer's disease. *Hum Genet* 131(7):1245–1249.
71. Abecasis GR, et al.; 1000 Genomes Project Consortium (2012) An integrated map of genetic variation from 1,092 human genomes. *Nature* 491(7422):56–65.
72. Rosenbloom KR, et al. (2015) The UCSC Genome Browser database: 2015 update. *Nucleic Acids Res* 43(Database issue):D670–D681.
73. Danecek P, et al.; 1000 Genomes Project Analysis Group (2011) The variant call format and VCFtools. *Bioinformatics* 27(15):2156–2158.
74. Cadzow M, et al. (2014) A bioinformatics workflow for detecting signatures of selection in genomic data. *Front Genet* 5:293.
75. Vitti JJ, Grossman SR, Sabeti PC (2013) Detecting natural selection in genomic data. *Annu Rev Genet* 47:97–120.
76. Song Y, Niu T, Manson JE, Kwiatkowski DJ, Liu S (2004) Are variants in the CAPN10 gene related to risk of type 2 diabetes? A quantitative assessment of population and family-based association studies. *Am J Hum Genet* 74(2):208–222.
77. Lyssenko V, et al. (2007) Mechanisms by which common variants in the TCF7L2 gene increase risk of type 2 diabetes. *J Clin Invest* 117(8):2155–2163.
78. Deelen J, et al. (2014) Genome-wide association meta-analysis of human longevity identifies a novel locus conferring survival beyond 90 years of age. *Hum Mol Genet* 23(16):4420–4432.
79. Cipollone F, et al.; Identification of New Elements of Plaque Stability (INES) Study Group (2004) A polymorphism in the cyclooxygenase 2 gene as an inherited protective factor against myocardial infarction and stroke. *JAMA* 291(18):2221–2228.
80. Thompson EE, et al. (2004) CYP3A variation and the evolution of salt-sensitivity variants. *Am J Hum Genet* 75(6):1059–1069.
81. Helbecque N, Cottel D, Codron V, Berr C, Amouyel P (2004) Paraoxonase 1 gene polymorphisms and dementia in humans. *Neurosci Lett* 358(1):41–44.
82. Weir BS, Cockerham CC (1984) Estimating F-statistics for the analysis of population structure. *Evolution* 38(6):1358–1370.
83. Tang K, Thornton KR, Stoneking M (2007) A new approach for using genome scans to detect recent positive selection in the human genome. *PLoS Biol* 5(7):e171.
84. Voight BF, Kudaravalli S, Wen X, Pritchard JK (2006) A map of recent positive selection in the human genome. *PLoS Biol* 4(3):e72.
85. Tajima F (1989) Statistical method for testing the neutral mutation hypothesis by DNA polymorphism. *Genetics* 123(3):585–595.
86. Fay JC, Wu CI (2000) Hitchhiking under positive Darwinian selection. *Genetics* 155(3): 1405–1413.

Supporting Information

Schwarz et al. 10.1073/pnas.1517951112

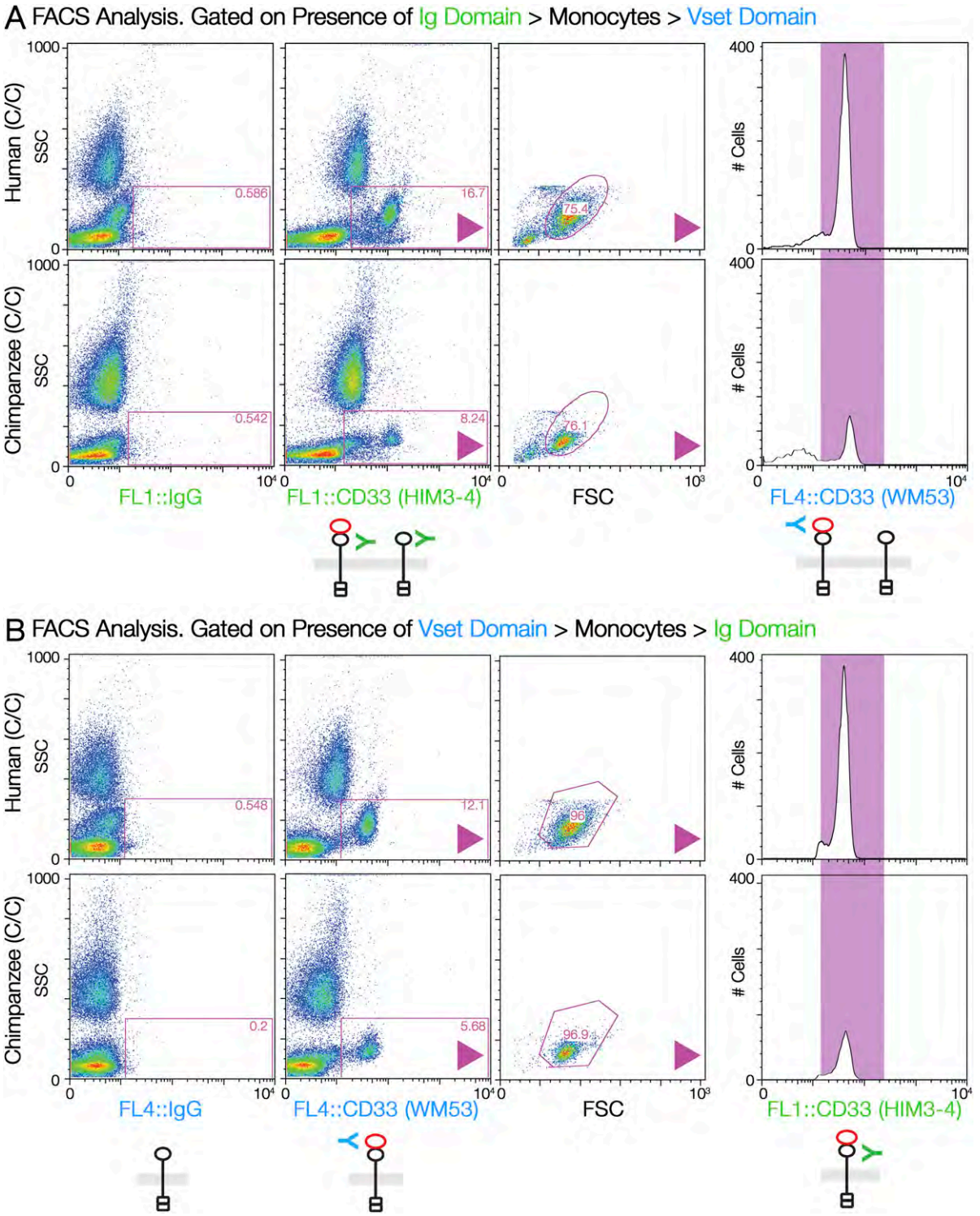

Fig. S1. Step-by-step analysis of CD33 expression in human and chimpanzee samples, using antibodies that bind to different Ig domains. The anti-CD33 antibodies clone HIM3-4 (depicted in green) binds to the second Ig domain, whereas the WM-53 clone (in blue) binds to the outermost V-set domain. (*A*) HIM3-4-positive cells (second panel) were gated to include monocytes (third panel), and then analyzed for binding to WM-53 (fourth panel). (*B*) WM-53-positive cells (second panel) were gated to include monocytes (third panel) and then analyzed for binding to HIM3-4 (fourth panel).

Dataset S1. Metrics of population structure, haplotype structure, and polymorphism distribution

Dataset S1

Population structure comparisons: F_{ST} (82). Haplotype structure within and between populations: Rsb and iHS (83, 84). Polymorphism distribution within populations: Tajima's D (85); Fay and Wu's H (86). Statistics are calculated using individuals from different geographic regions, as defined in the 1000 Genomes dataset.

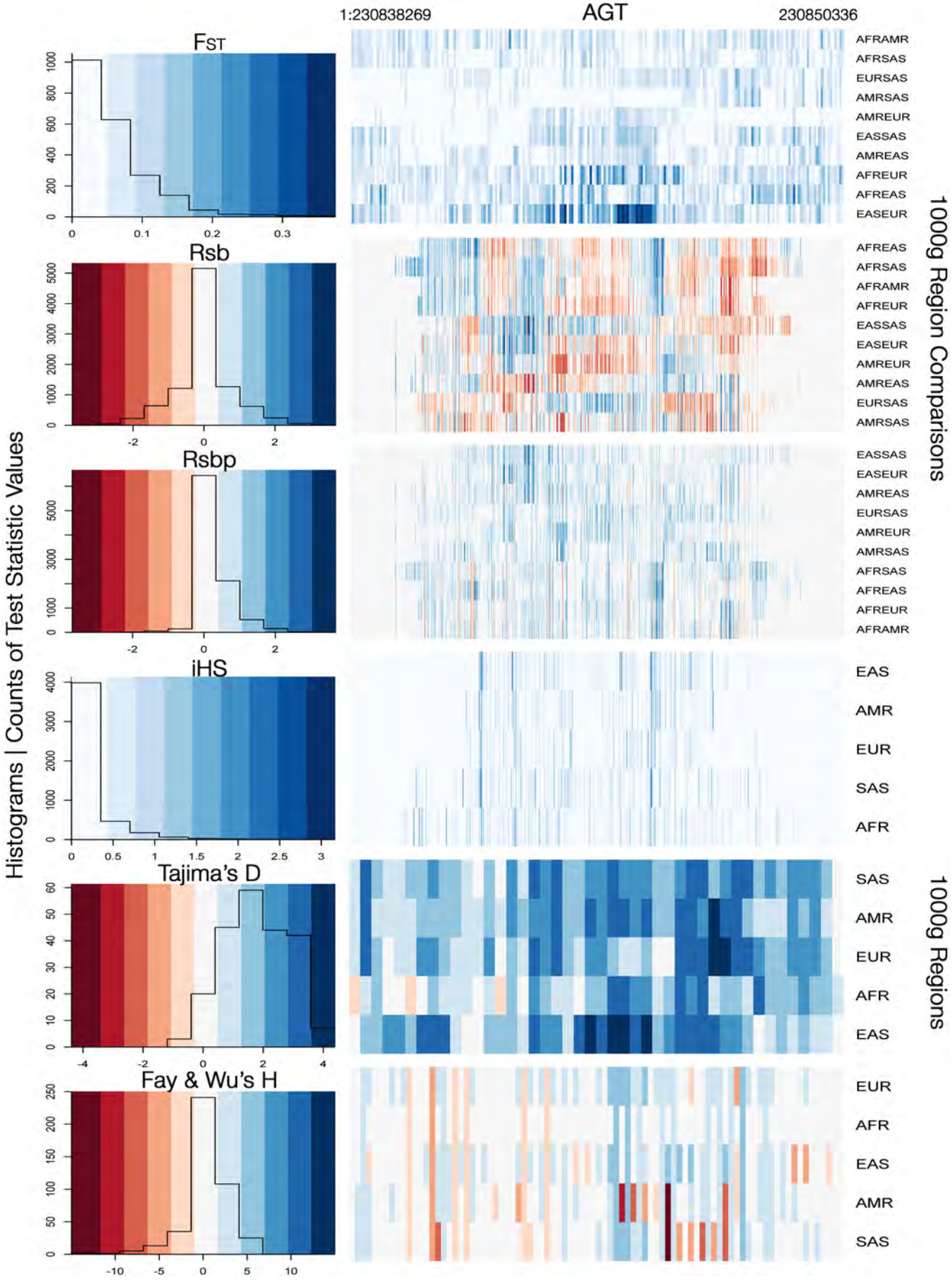
1:230838269
AGT
230850336
FST
Rsb
Rsbp
iHS
Tajima's D
Fay & Wu's H
Histograms | Counts of Test Statistic Values
AFRAMR
AFRSAS
EURSAS
AMRSAS
AMREUR
EASSAS
AMREAS
AFREUR
AFREAS
EASEUR
1000g Region Comparisons
AFREAS
AFRSAS
AFRAMR
AFREUR
EASSAS
EASEUR
AMREUR
AMREAS
EURSAS
AMRSAS
EASSAS
EASEUR
AMREAS
EURSAS
AMREUR
AMRSAS
AFRSAS
AFREAS
AFREUR
AFRAMR
EAS
AMR
EUR
SAS
AFR
SAS
AMR
EUR
AFR
EAS
1000g Regions
EUR
AFR
EAS
AMR
SAS

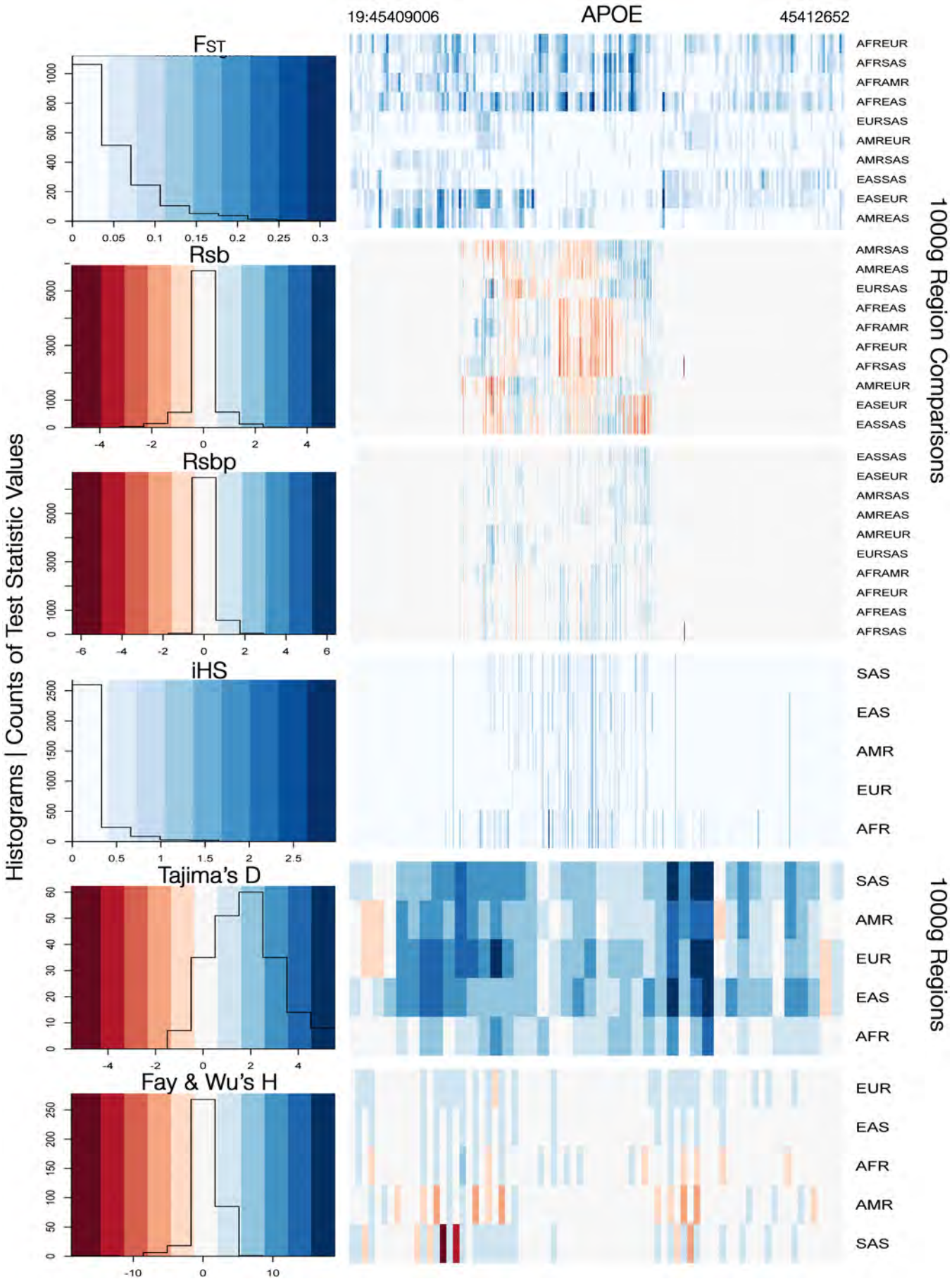
19:45409006
APOE
45412652
FST
Rsb
Rsbp
iHS
Tajima's D
Fay & Wu's H
Histograms | Counts of Test Statistic Values
AFREUR
AFRSAS
AFRAMR
AFREAS
EURSAS
AMREUR
AMRSAS
EASSAS
EASEUR
AMREAS
1000g Region Comparisons
SAS
EAS
AMR
EUR
AFR
1000g Regions

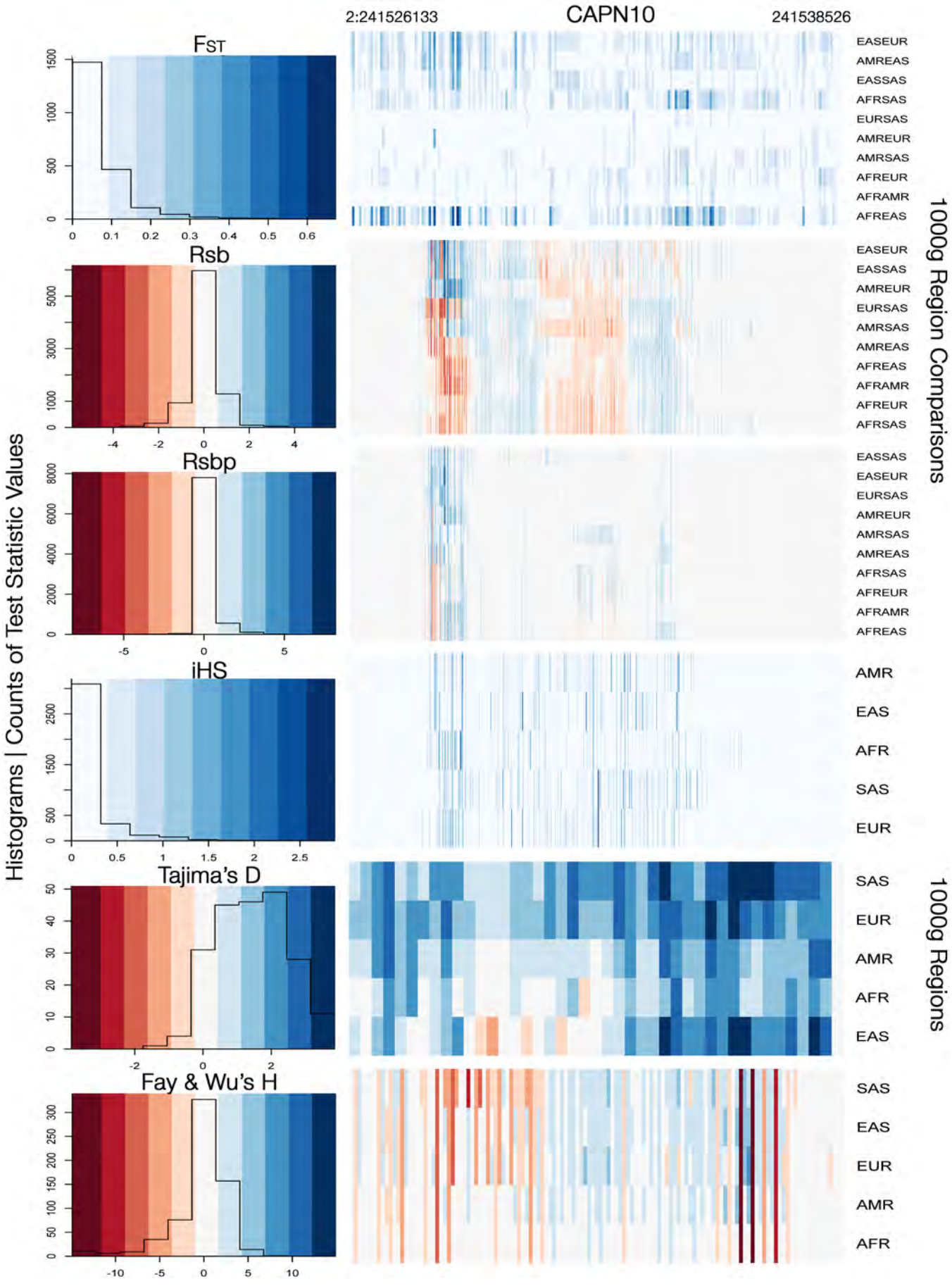
2:241526133
CAPN10
241538526
FST
Rsb
Rsbp
iHS
Tajima's D
Fay & Wu's H
Histograms | Counts of Test Statistic Values
1000g Region Comparisons
1000g Regions
EASEUR
AMREAS
EASSAS
AFRSAS
EURSAS
AMREUR
AMRSAS
AFREUR
AFRAMR
AFREAS
AMR
EAS
AFR
SAS
EUR

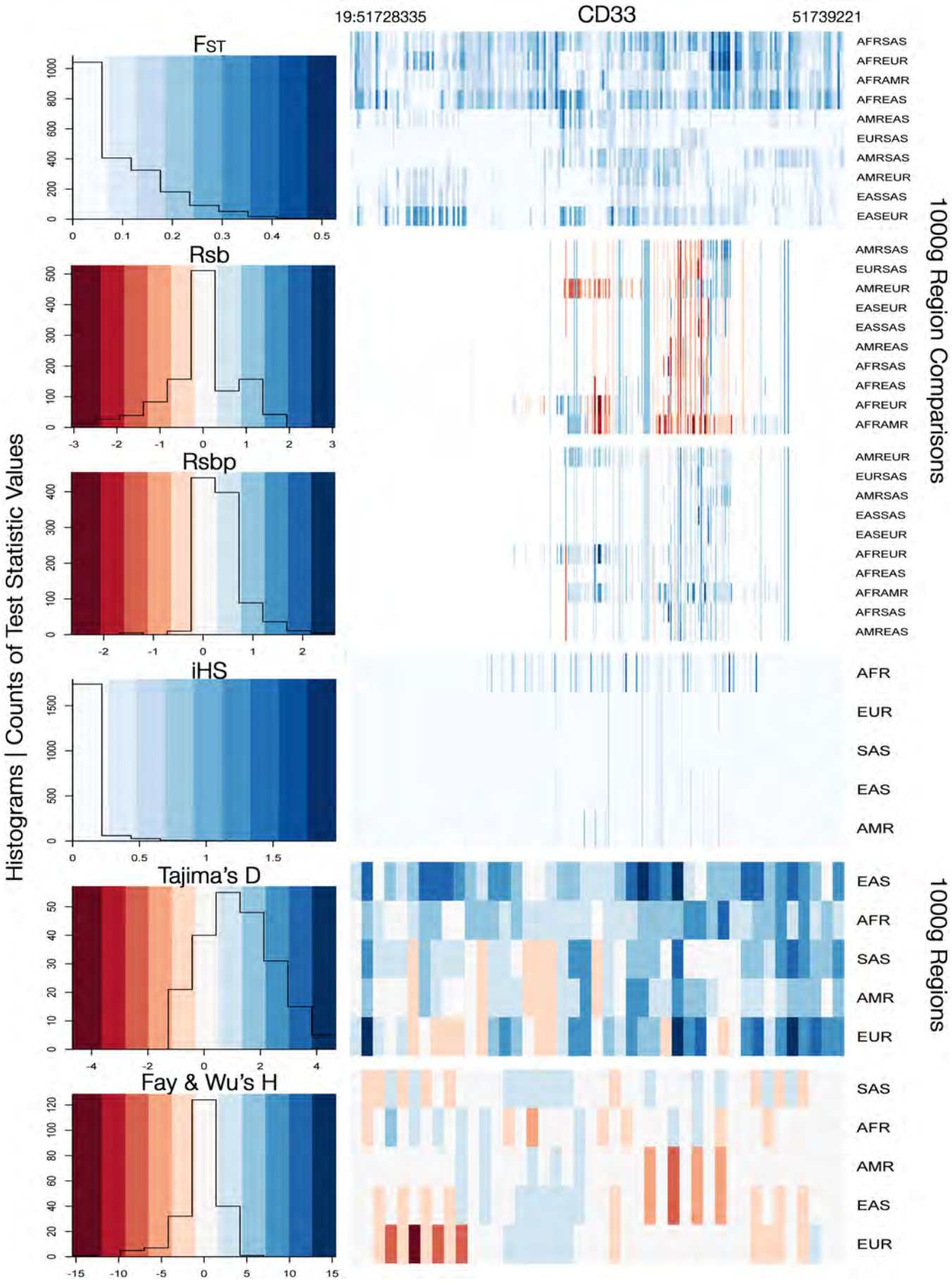
19:51728335
CD33
51739221
FST
Rsb
Rsbp
iHS
Tajima's D
Fay & Wu's H
Histograms | Counts of Test Statistic Values
1000g Region Comparisons
1000g Regions
AFRSAS
AFREUR
AFRAMR
AFREAS
AMREAS
EURSAS
AMRSAS
AMREUR
EASSAS
EASEUR
AFR
EUR
SAS
EAS
AMR

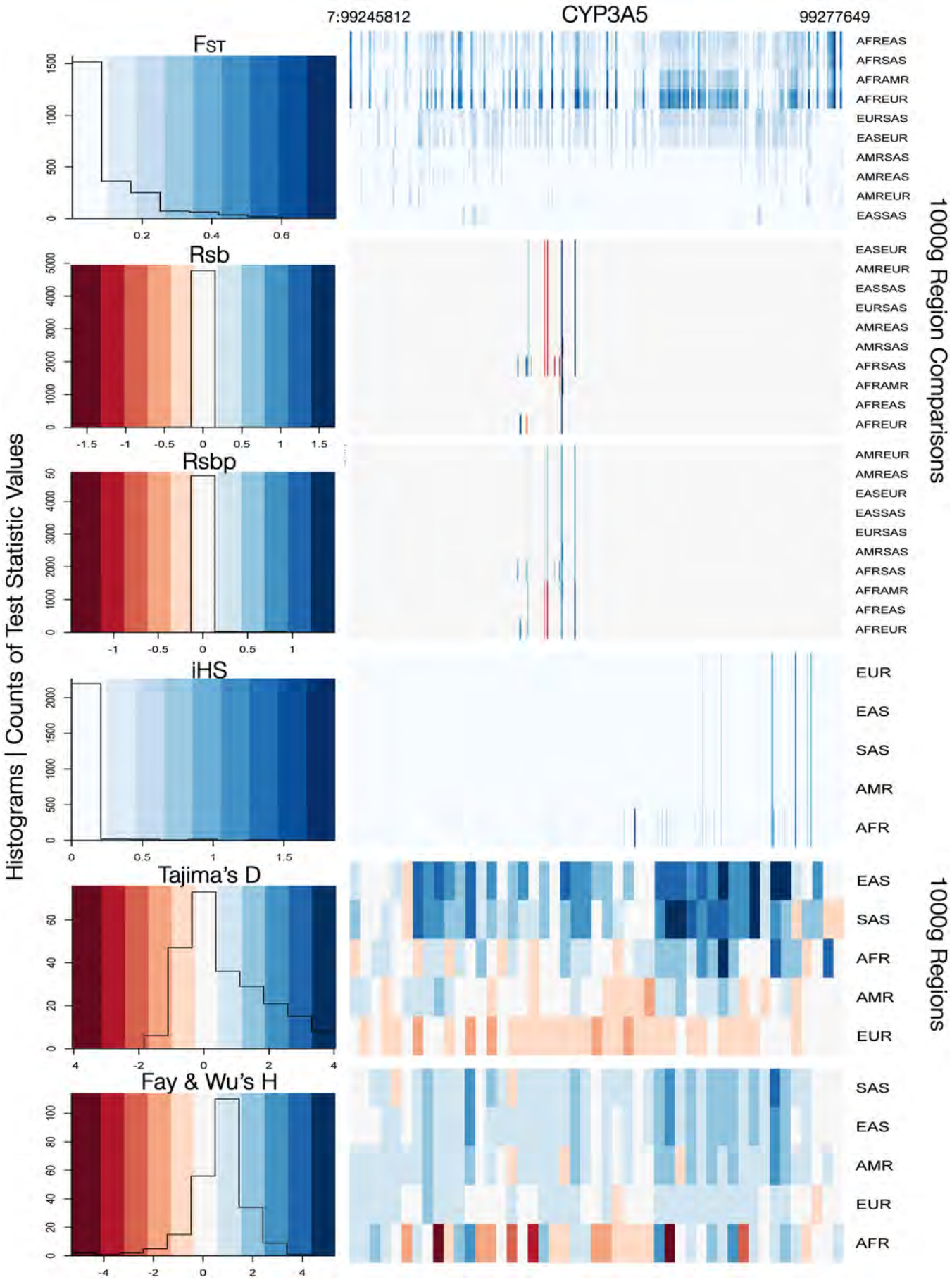
7:99245812
CYP3A5
99277649
FST
Rsb
Rsbp
iHS
Tajima's D
Fay & Wu's H
Histograms | Counts of Test Statistic Values
1000g Region Comparisons
1000g Regions
AFREAS
AFRSAS
AFRAMR
AFREUR
EURSAS
EASEUR
AMRSAS
AMREAS
AMREUR
EASSAS
EUR
EAS
SAS
AMR
AFR

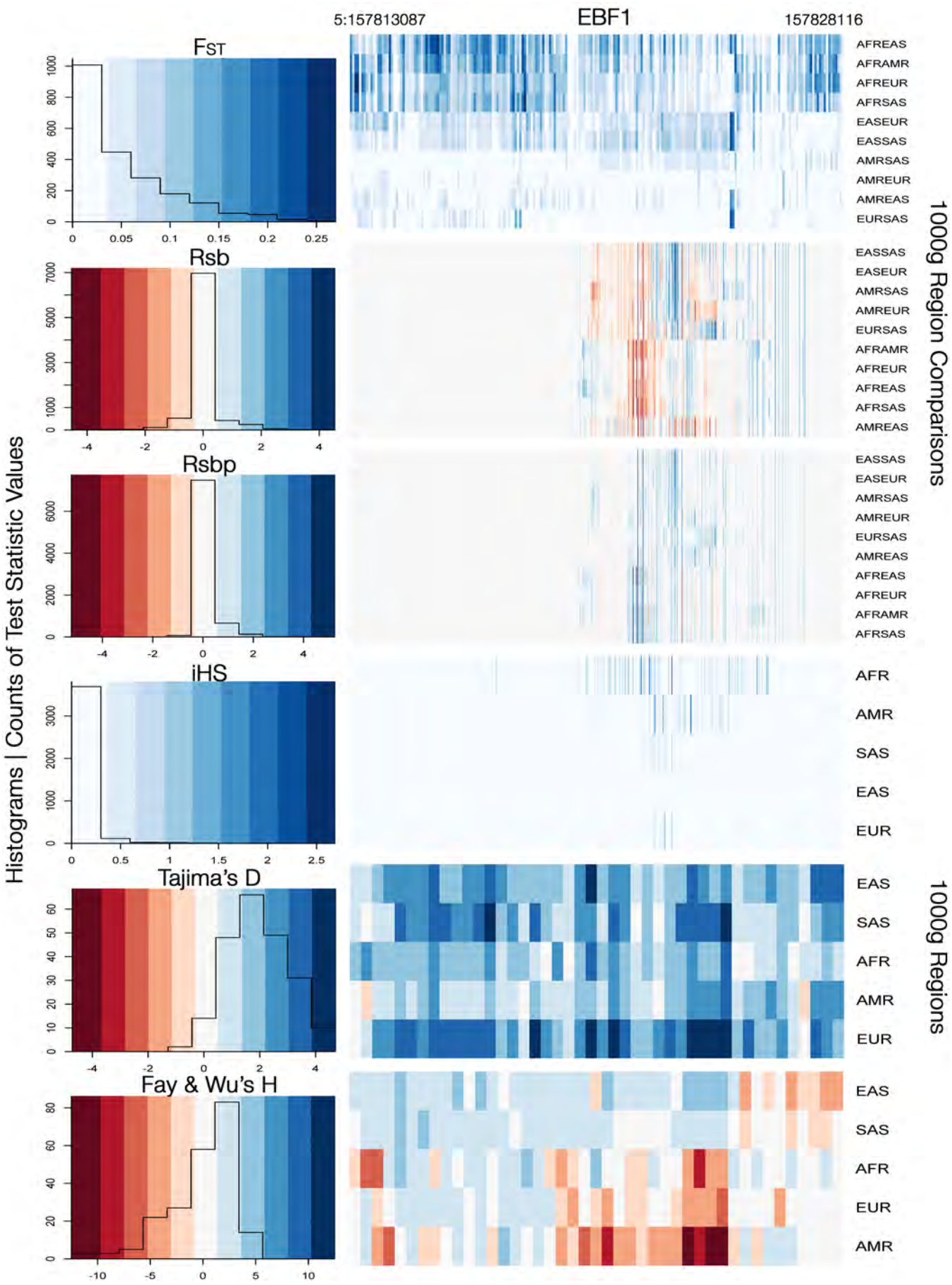
5:157813087
EBF1
157828116
FST
Rsb
Rsbp
iHS
Tajima's D
Fay & Wu's H
Histograms | Counts of Test Statistic Values
1000g Region Comparisons
1000g Regions
AFREAS
AFRAMR
AFREUR
AFRSAS
EASEUR
EASSAS
AMRSAS
AMREUR
AMREAS
EURSAS
AFR
AMR
SAS
EAS
EUR

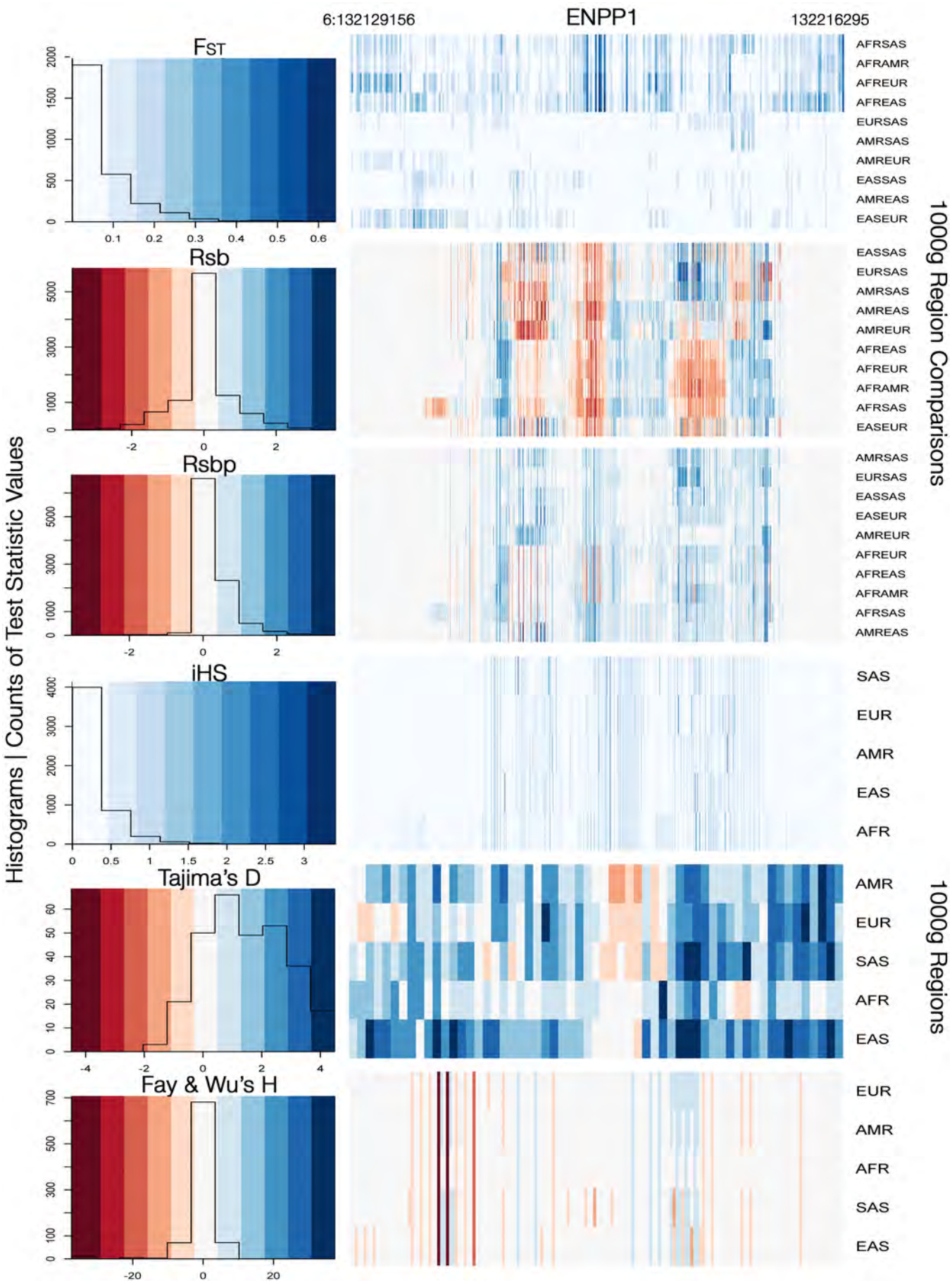
6:132129156
ENPP1
132216295
FST
Rsb
Rsbp
iHS
Tajima's D
Fay & Wu's H
Histograms | Counts of Test Statistic Values
AFRSAS
AFRAMR
AFREUR
AFREAS
EURSAS
AMRSAS
AMREUR
EASSAS
AMREAS
EASEUR
1000g Region Comparisons
SAS
EUR
AMR
EAS
AFR
1000g Regions

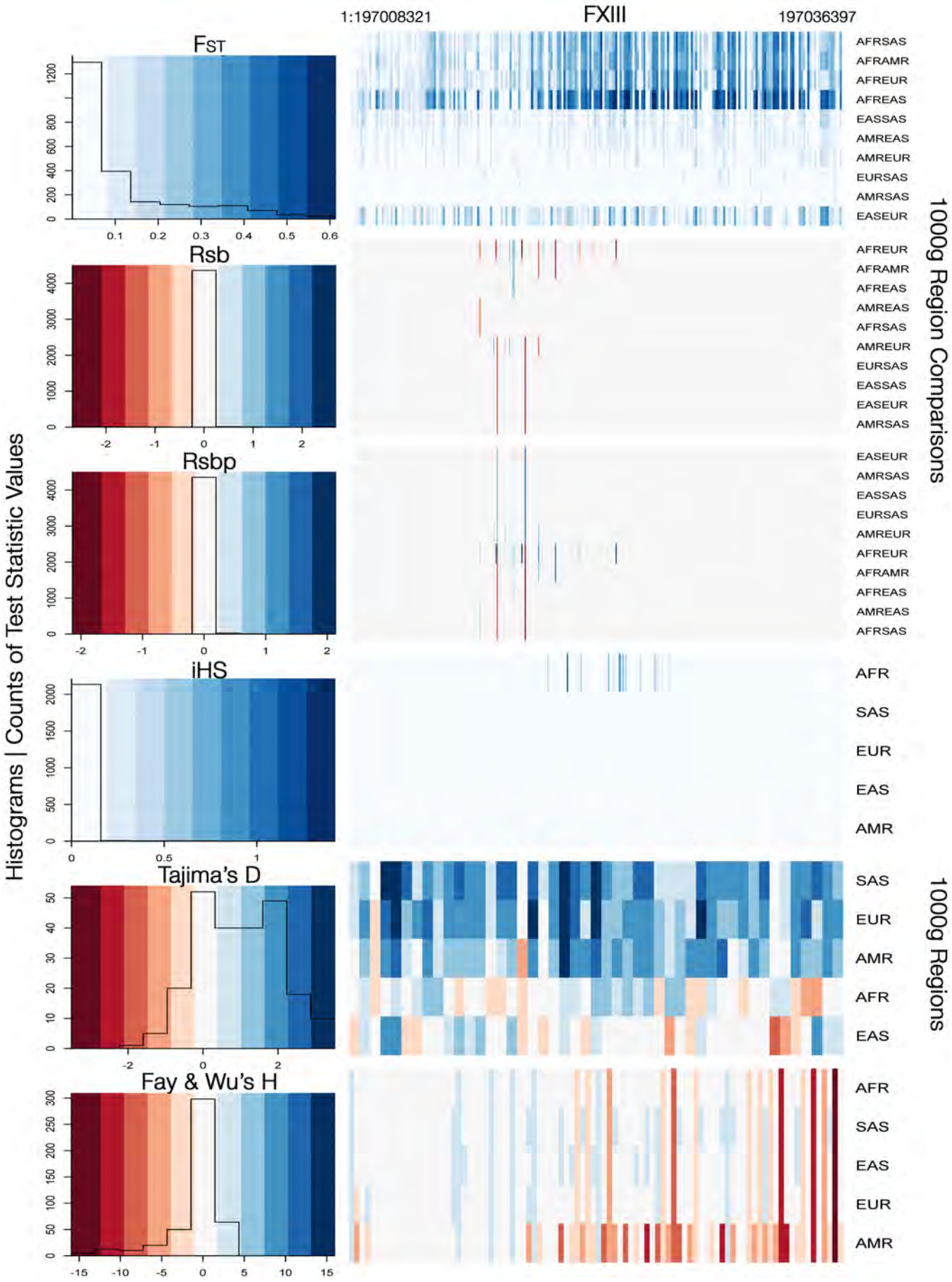
1:197008321
FXIII
197036397
FST
Rsb
Rsbp
iHS
Tajima's D
Fay & Wu's H
Histograms | Counts of Test Statistic Values
1000g Region Comparisons
1000g Regions
AFRSAS
AFRAMR
AFREUR
AFREAS
EASSAS
AMREAS
AMREUR
EURSAS
AMRSAS
EASEUR
AFR
SAS
EUR
EAS
AMR

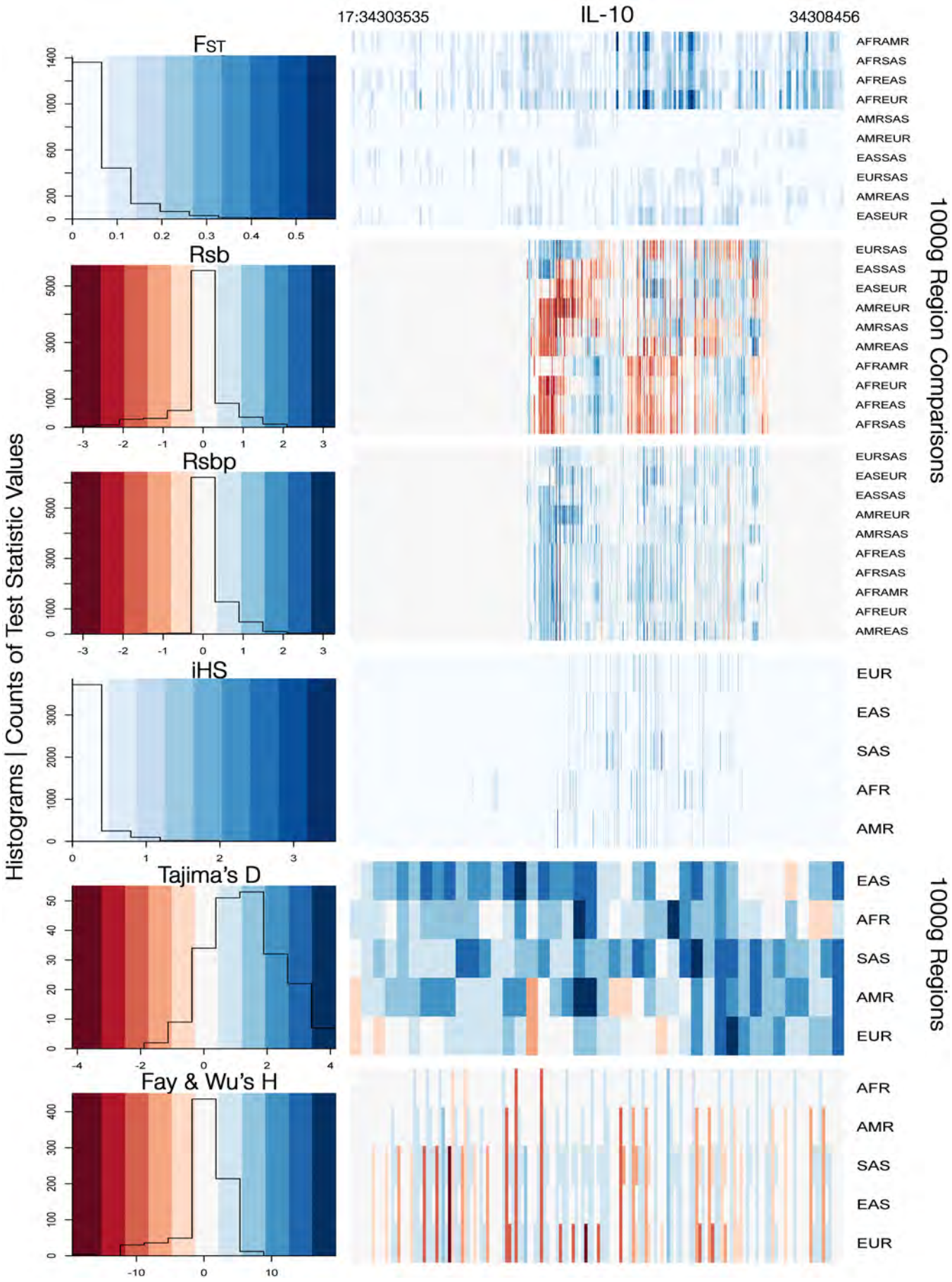
17:34303535
IL-10
34308456
Histograms | Counts of Test Statistic Values
FST
Rsb
Rsbp
iHS
Tajima's D
Fay & Wu's H
1000g Region Comparisons
1000g Regions
AFRAMR
AFRSAS
AFREAS
AFREUR
AMRSAS
AMREUR
EASSAS
EURSAS
AMREAS
EASEUR
EUR
EAS
SAS
AFR
AMR

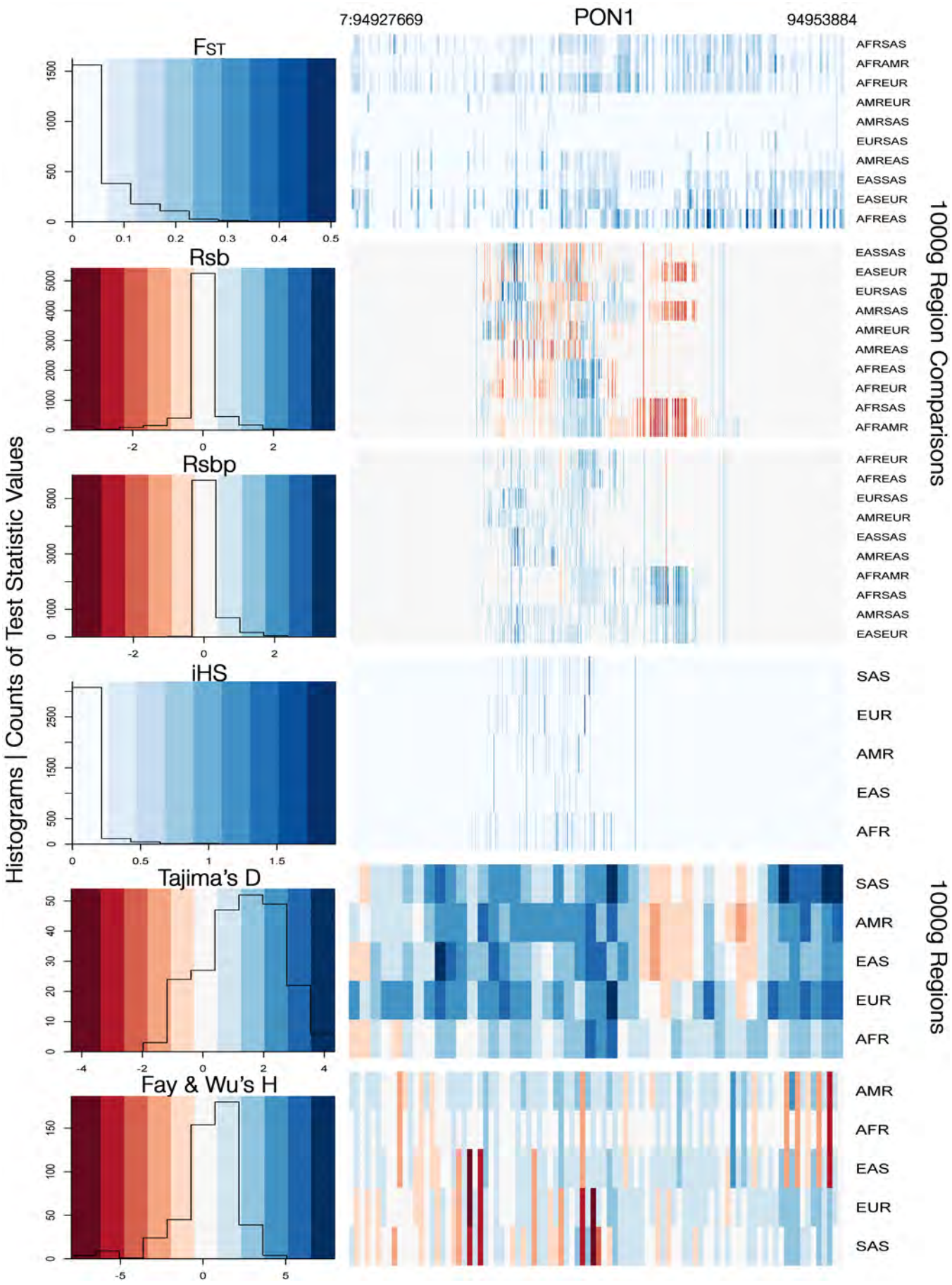
7:94927669
PON1
94953884
FST
Rsb
Rsbp
iHS
Tajima's D
Fay & Wu's H
Histograms | Counts of Test Statistic Values
1000g Region Comparisons
1000g Regions
AFRSAS
AFRAMR
AFREUR
AMREUR
AMRSAS
EURSAS
AMREAS
EASSAS
EASEUR
AFREAS
SAS
EUR
AMR
EAS
AFR

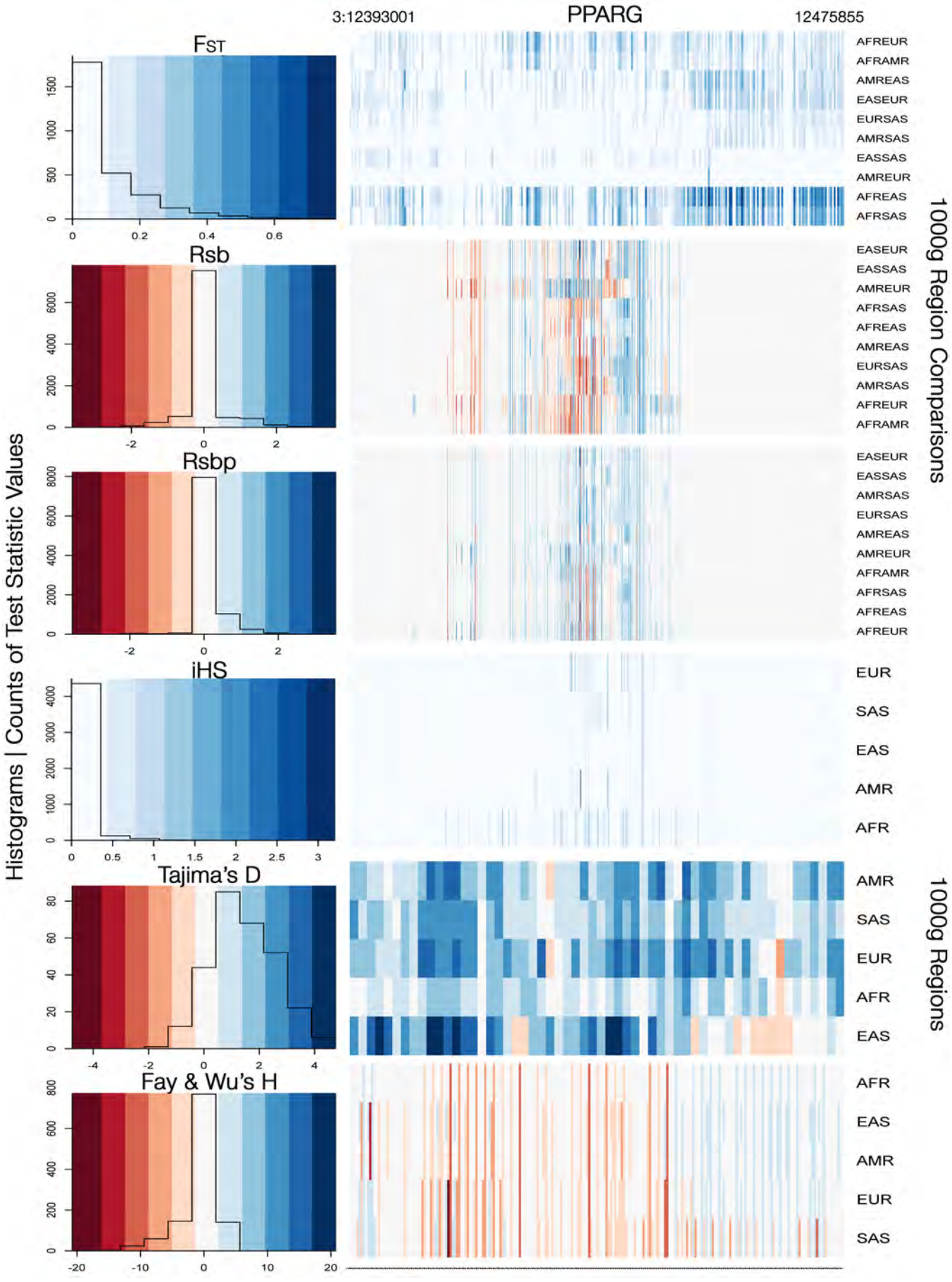
3:12393001
PPARG
12475855
FST
Rsb
Rsbp
iHS
Tajima's D
Fay & Wu's H
Histograms | Counts of Test Statistic Values
1000g Region Comparisons
1000g Regions
AFREUR
AFRAMR
AMREAS
EASEUR
EURSAS
AMRSAS
EASSAS
AMREUR
AFREAS
AFRSAS
EUR
SAS
EAS
AMR
AFR

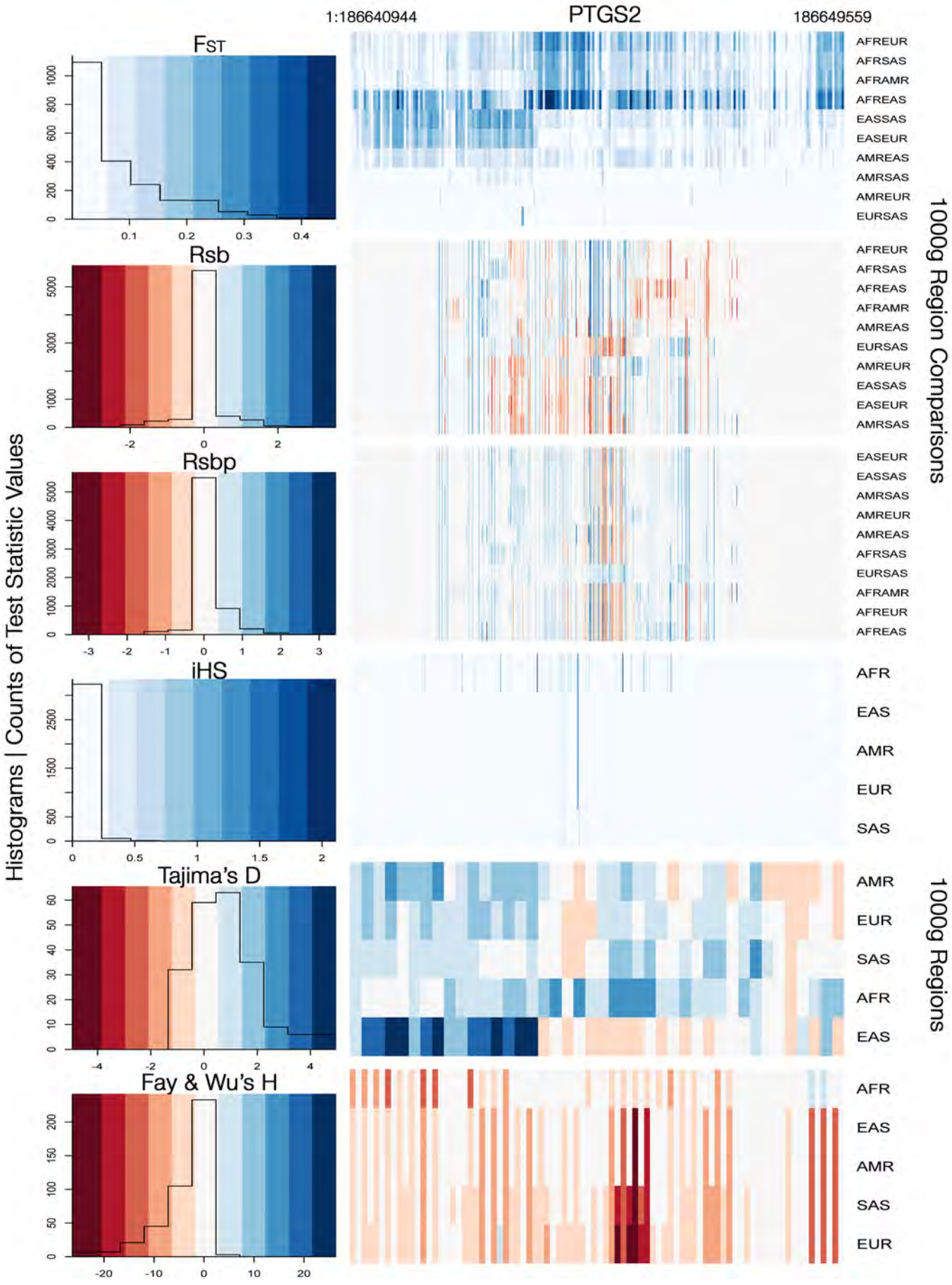
1:186640944
PTGS2
186649559
FST
Rsb
Rsbp
iHS
Tajima's D
Fay & Wu's H
Histograms | Counts of Test Statistic Values
1000g Region Comparisons
1000g Regions
AFREUR
AFRSAS
AFRAMR
AFREAS
EASSAS
EASEUR
AMREAS
AMRSAS
AMREUR
EURSAS
AFR
EAS
AMR
EUR
SAS

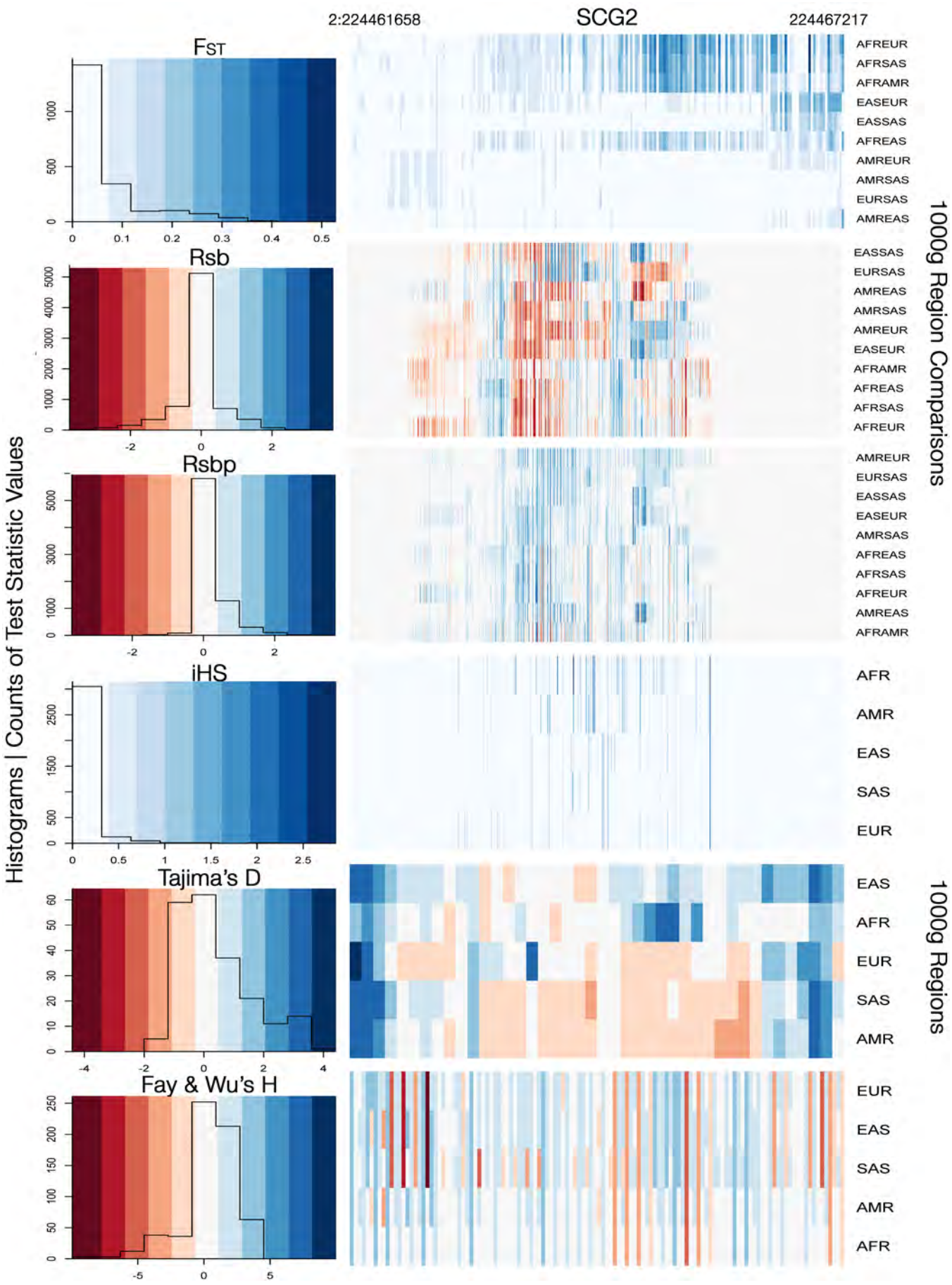
2:224461658
SCG2
224467217
FST
Rsb
Rsbp
iHS
Tajima's D
Fay & Wu's H
Histograms | Counts of Test Statistic Values
AFREUR
AFRSAS
AFRAMR
EASEUR
EASSAS
AFREAS
AMREUR
AMRSAS
EURSAS
AMREAS
1000g Region Comparisons
AFR
AMR
EAS
SAS
EUR
1000g Regions

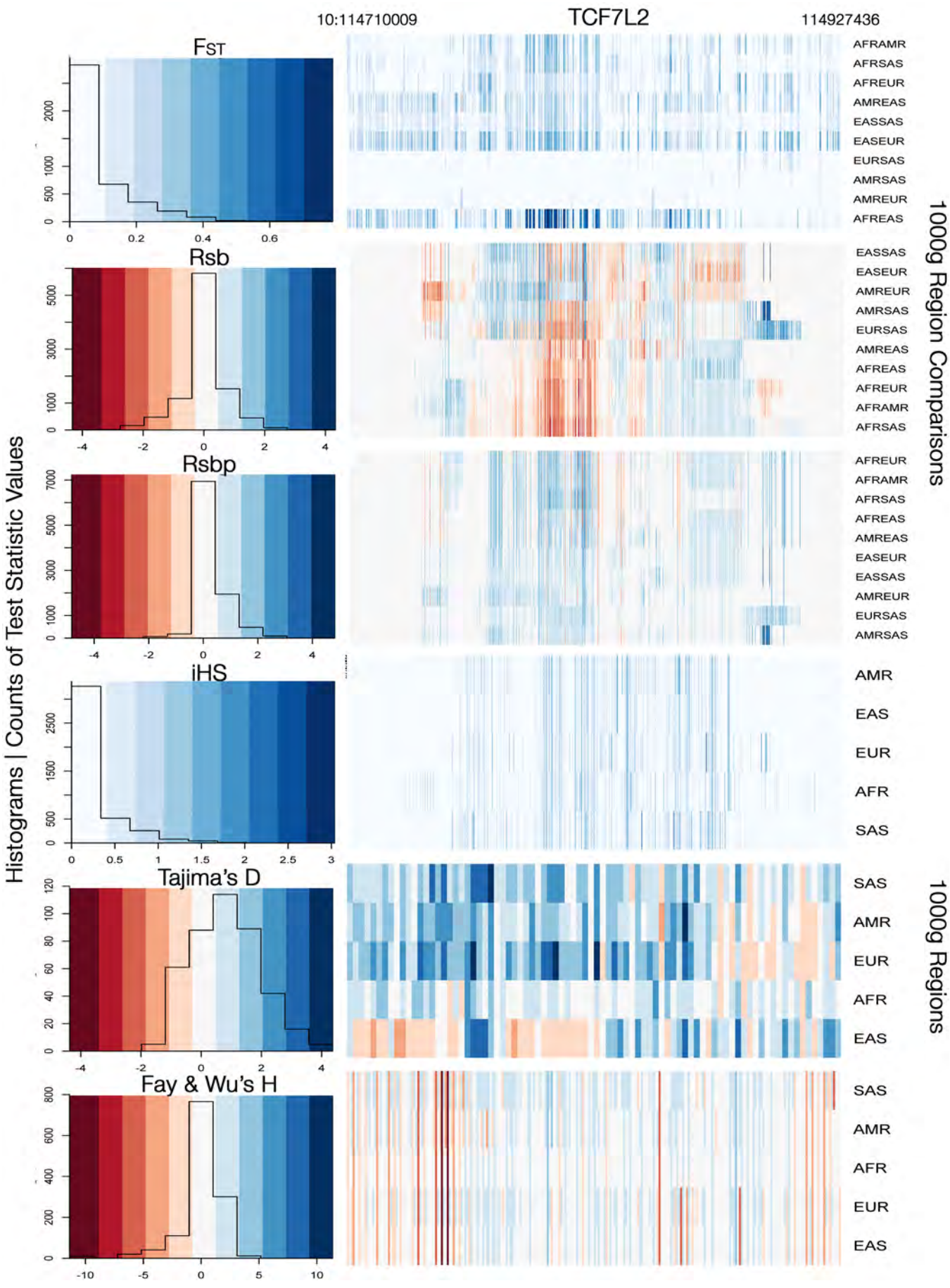
10:114710009
TCF7L2
114927436
FST
Rsb
Rsbp
iHS
Tajima's D
Fay & Wu's H
Histograms | Counts of Test Statistic Values
1000g Region Comparisons
1000g Regions
AFRAMR
AFRSAS
AFREUR
AMREAS
EASSAS
EASEUR
EURSAS
AMRSAS
AMREUR
AFREAS
AMR
EAS
EUR
AFR
SAS